

Variable refractory lithophile element compositions of planetary building blocks: insights from components of enstatite chondrites

Takashi Yoshizaki^{*1}, Richard D. Ash², Marc D. Lipella^{†2}, Tetsuya Yokoyama³, and
William F. McDonough^{1,2,4}

¹Department of Earth Science, Graduate School of Science, Tohoku University, Sendai,
Miyagi 980-8578, Japan

²Department of Geology, University of Maryland, College Park, MD 20742, USA

³Department of Earth and Planetary Sciences, Tokyo Institute of Technology, Ookayama,
Tokyo 152-8851, Japan

⁴Research Center of Neutrino Sciences, Tohoku University, Sendai, Miyagi 980-8578,
Japan

June 1, 2021

^{*}Corresponding author. E-mail: tky@dc.tohoku.ac.jp

[†]Deceased.

Abstract

Chondrites are sediments of materials left over from the earliest stage of the solar system history. Based on their undifferentiated nature and less fractionated chemical compositions, chondrites are widely considered to represent the unprocessed building blocks of the terrestrial planets and their embryos. Models of chemical composition of the terrestrial planets generally find chondritic relative abundances of refractory lithophile elements (RLE) in the bulk bodies ("constant RLE ratio rule"), based on limited variations of RLE ratios among chondritic meteorites and the solar photosphere. Here, we show that ratios of RLE, such as Nb/Ta, Zr/Hf, Sm/Nd and Al/Ti, are fractionated from the solar value in chondrules from enstatite chondrites (EC). The fractionated RLE ratios of individual EC chondrules document different chalcophile affinities of RLE under highly reducing environments and a separation of RLE-bearing sulfides from silicates before and/or during chondrule formation. In contrast, the bulk EC have solar-like RLE ratios, indicating that a physical sorting of silicates and sulfides was negligible before and during the accretion of EC parent bodies. Likewise, if the Earth's accretion were dominated by EC-like materials, as supported by multiple isotope systematics, the physical sorting of silicates and sulfides in the accretionary disk should not have occurred among the Earth's building blocks. Alternatively, the Earth's precursors might have been high-temperature nebular materials that condensed before the RLE fractionation due to precipitation of the RLE-bearing sulfides. A lack of Ti depletion in the bulk silicate Earth, combined with similar silicate-sulfide and rutile-melt partitioning behaviors of Nb and Ti, prefers a moderately siderophile behavior of Nb as the origin of the accessible Earth's Nb depletion. Highly reduced planets that have experienced selective removal or accretion of silicates or metal/sulfide phases, such as Mercury, might have fractionated, non-solar bulk RLE ratios.

Keywords: planets, chondrites, Earth, refractory lithophile elements, chemical fractionation

1 Introduction

The geochemical classification of elements is established based on their partitioning behaviors during condensation into a silicate (lithophile), metal (siderophile) or sulfide (chalcophile) phases (e.g., Lodders, 2003). Elements are also classified cosmochemically based on their volatilities. There are 36 refractory elements, and most of them are generally considered to be lithophile (e.g., Be, Al, Ca, Ti, Sc, Sr, Y, Zr, Nb, Ba, rare earth elements (REE), Hf, Ta, Th and U), while V, Mo, and W are moderately siderophile/chalcophile, and Ru, Rh, Re, Os, Ir, and Pt are highly siderophile. Chondritic meteorites (chondrites) are undifferentiated solar system materials that are widely considered as planetary building blocks. The relative abundances of the most refractory lithophile elements (RLE) are nearly constant ($\lesssim 10\%$) for the solar photosphere and among chondritic meteorites (Larimer and Wasson, 1988; Wasson and Kallemeyn, 1988; Bouvier et al., 2008). Importantly, compositional models of Earth (Allègre et al., 1995; McDonough and Sun, 1995; Palme and O'Neill, 2014) and Mars (Wänke and Dreibus, 1994; Yoshizaki and McDonough, 2020) commonly find or assume chondritic RLE ratios (e.g., Ca/Al, Sm/Nd, Lu/Hf, Th/U) for these planets ("constant RLE ratio rule").

However, recent high-precision measurements of chondritic and terrestrial samples revealed detectable variations of not only REE ratios (Dauphas and Pourmand, 2015; Barrat et al., 2016), but also geochemical twins' ratios such as Y/Ho (Pack et al., 2007), Zr/Hf (Patzer et al., 2010), and Nb/Ta (Münker et al., 2003) among these solar system materials. For example, the observation of lower Nb/Ta of the accessible Earth as compared to CI chondrites, which show the closest match to the solar photosphere composition for many elements (e.g., Lodders, 2020), raised considerable discussions on their relative behaviors. Some authors proposed that Nb and Ta are exclusively lithophile and hosted in a eclogitic reservoir hidden in the mantle (Sun and McDonough, 1989; McDonough, 1991; Kamber and Collerson, 2000; Rudnick et al., 2000; Nebel et al., 2010), whereas

others have suggested that Nb and less so Ta behaved as moderately siderophile (Wade and Wood, 2001; Münker et al., 2003; Corgne et al., 2008; Mann et al., 2009; Cartier et al., 2014) or chalcophile (Münker et al., 2017) elements and have been partially sequestered into the metallic core.

The Earth's specific building blocks remain unknown. Among chondritic meteorites, enstatite chondrites (EC) show the closest matches to the Earth's mantle in multiple isotopic systematics (Javoy et al., 2010; Warren, 2011; Dauphas, 2017; Boyet et al., 2018). On the other hand, EC are characterized by lower Mg/Si and RLE/Mg ratios and higher volatile abundances as compared to Earth (Palme et al., 1988; McDonough and Sun, 1995). EC are rare type of chondrite in our collection that record the most reducing conditions among chondritic meteorites (Fig. 1; Keil, 1968; Larimer, 1968). The chemical and isotopic composition of meteorites and Earth, combined with partitioning behaviors of elements, indicate that an early stage of the Earth's formation was dominated by an accretion of EC-like, highly reduced materials, followed by an accretion of less reduced ones (e.g., Corgne et al., 2008; Mann et al., 2009; Schönbächler et al., 2010; Rubie et al., 2011, 2015). It is known that multiple RLE show non-lithophile behaviors under highly reduced conditions as recorded in EC (e.g., Barrat et al., 2014; Münker et al., 2017), but contributions of such characteristics of RLE to the compositions of Earth and its building blocks remain poorly understood.

Here, we report RLE composition of chondrules, one of the major RLE carriers in chondritic meteorites (e.g., Alexander, 2005, 2019a,b) and potential dominant source materials of the terrestrial mantle (e.g., Hewins and Herzberg, 1996; Johansen et al., 2015; Levison et al., 2015; Amsellem et al., 2017; Yoshizaki and McDonough, 2021), and sulfides from primitive EC samples, to reveal non-lithophile behavior of RLE in highly reducing environments. Using these and published data from different types of chondrites, combined with some new RLE data for refractory inclusions from carbonaceous chondrites (CC), we examine a compositional variability in RLE ratios within the accretionary disk, behavior of elements under variable redox conditions, and the chondritic reference

frame for bulk planetary compositions.

2 Samples and methods

2.1 Samples

In order to reduce potential modifications of elemental abundances by parent body metamorphism and terrestrial weathering, we chose unequilibrated (type 3) EH, EL and CV chondrites with limited terrestrial weathering as samples for this study (Table 1). Analyses were conducted on 92 chondrules, 40 troilites (FeS), 9 oldhamites (CaS) and 5 niningerites (MgS) from Alan Hills (ALH) A77295 (EH3), ALH 84170 (EH3), ALH 84206 (EH3), ALH 85119 (EL3) and MacAlpine Hills (MAC) 88136 (EL3). We also studied two Ca, Al-rich inclusions (CAI) from Allende (CV3), and one CAI and six amoeboid olivine aggregates (AOA) from Roberts Massif (RBT) 04143 (CV3). The petrology and mineralogy of these meteorites have been well characterized in previous studies (e.g., Johnson and Lofgren, 1995; Rubin et al., 1997; Benoit et al., 2002; Lin and El Goresy, 2002; Grossman and Brearley, 2005; Gannoun et al., 2011; Quirico et al., 2011; Ishida et al., 2012; Yoshizaki et al., 2019; Bonal et al., 2020).

2.2 Analytical methods

Mineralogy, petrology and major element compositions of polished sections of the samples were analyzed using scanning electron microscopes (SEM) and electron probe microanalyzers (EPMA) at Tohoku University and University of Maryland, using procedures after Yoshizaki et al. (2019; Section B.1). Trace element compositions of chondritic components were determined using a New Wave frequency-quintupled Nd:YAG laser system coupled to a Thermo Finnigan Element2 single-collector ICP-MS at University of Maryland, following procedures of Lehner et al. (2014). Operating conditions are summarized in Table 2. Measurements were carried out in low-mass resolution

mode ($M/\Delta M = 300$), with 15–200 μm laser spot size and a fluence of $\sim 2\text{--}3 \text{ J/cm}^2$. In all circumstances, the spot size was set to be smaller than the chondrule so that the laser sampled only the polymineralic interiors of chondrules. The beam was focused onto a sample placed in a 3 cm^3 ablation cell, which was continuously flushed to the plasma source of the mass spectrometer with a He gas flow of $\sim 1 \text{ L/min}$. The mass spectrometer was tuned to maximize signal (based on ^{43}Ca and ^{232}Th spectra) and minimize oxide production ($\text{UO}/\text{U} < 1.2\%$) to maximize sensitivity and reduce polyatomic interference. A dwell time of 5–15 milliseconds was used depending on element concentrations. After the LA-ICP-MS measurements, the sampled areas were investigated using SEM, to make sure that there was no contamination due to beam overlapping onto neighboring phases (e.g., matrix).

In LA-ICP-MS measurement of chondrules and refractory inclusions, National Institute of Standards and Technology (NIST) 610 glass (Jochum et al., 2011) was used as an external standard material. Internal standards were ^{29}Si for chondrules, and ^{29}Si , ^{43}Ca or ^{47}Ti for refractory inclusions, which were determined as a polymineralic bulk composition using EPMA. For sulfides, the group IIA iron meteorite Filomena (for siderophile elements) and the NIST 610 glass (for lithophile elements) were used as reference materials, using data from Walker et al. (2008) and the GeoReM database (Jochum et al., 2011) as working values, respectively. Count rates were normalized using ^{57}Fe (for Filomena) and ^{63}Cu (for NIST 610) as internal standards, which were determined using EPMA or SEM/EDS. The standard materials were measured at least twice at the start of individual analytical run that is composed of 16 analyses of unknown samples. All obtained data were processed using the LAMTRACE software (van Achterbergh et al., 2001). Data with a potential beam overlapping onto neighboring phases were rejected in this procedure. The long-term reproducibilities of isotope ratios for the external standards were better than 5% for nearly all of the measured elements, except for Ni and Cu in Filomena (Table B.1). We also routinely measured the BHVO-2G glass as a secondary standard material in order to monitor accuracy of the analysis, which well

reproduced the preferred values (Jochum and Nohl, 2008) within $<5\%$. We report mean ± 2 standard errors of the mean ($2\sigma_m$) of RLE ratios of EC chondrules, EC sulfides, and CC refractory inclusions, as a measure of their average RLE ratios.

3 Results

3.1 Chondrules from unequilibrated enstatite chondrites

Various types of chondrules are identified and measured in this study. More than 70% of them are porphyritic pyroxene (PP) chondrules, with less abundant ($\sim 15\%$) radial pyroxene (RP), olivine-bearing (porphyritic olivine pyroxene (POP) or porphyritic olivine (PO) type; $\sim 10\%$), and other rare types (Figs. 2 and 3). These chondrules are mostly 200–600 μm in diameter, with some reaching up to 1 mm. The observed abundance of chondrule types and their size distributions are consistent with previous reports (e.g., Jones, 2012; Weisberg and Kimura, 2012; Jacquet et al., 2018).

PP chondrules are mainly composed of Fe-poor (<2 wt%) enstatite and mesostasis, with minor silicates such as olivine and silica, as reported by previous studies (e.g., Weisberg and Kimura, 2012; Jacquet et al., 2018). They sometimes contain small amounts of opaque phases, such as Si-bearing Fe-Ni metal, troilite, oldhamite, niningerite (only in EH3) and alabandite (MnS; only in EL3). Although each PP chondrule shows variable lithophile element abundances, with absolute RLE enrichment factors of 0.5–2 \times CI (Fig. 2A–E), their average compositions are similar in each sample (Fig. 2F). On average, PP chondrules are characterized by depletions of REE, Y, high-field strength elements (HFSE: Ti, Zr, Hf, Nb, Ta), Cr, Mn and K compared to Al, Mg and Si. REE and HFSE are also fractionated within these groups; Eu and Yb are depleted compared to other REE, and Zr and Nb show stronger depletions than their geochemical twins, Hf and Ta, respectively. One PP chondrule from MAC 88136 (C14) has numerous tiny grains of oldhamite in its glassy area, which might have contributed its elevated bulk REE and Y abundances.

Compared to PP chondrules, RP chondrules show lower RLE abundance ($0.2\text{--}1 \times \text{CI}$; Fig. 3A,B), whereas PO and POP chondrules have higher RLE abundances ($0.8\text{--}4 \times \text{CI}$; Fig. 3C). One cryptocrystalline chondrule shows flat RLE pattern with a strong negative Eu anomaly and Al, Mg and Si enrichments (Fig. 3D). In general, RP, olivine-bearing, and cryptocrystalline chondrules are enriched in Al, Mg and Si compared to most RLE and Cr, Mn and K, as observed in PP chondrules. We note that these variations are potentially affected by sectioning effects (see Section B.2). A Ca-px-rich chondrule in ALH 84206 shows a flat, elevated RLE pattern ($\sim 6 \times \text{CI}$), with clear depletions of Ce, Ba, Cr, Mn and K (Fig. 3D). In addition, EC chondrules show Mg/Si (0.84 ± 0.01 , $2\sigma_m$), which is lower than those of CI (0.89 ; Lodders, 2020) and the bulk silicate Earth (BSE) (1.1 ; McDonough and Sun, 1995; Palme and O'Neill, 2014).

EC chondrules show highly variable, fractionated ratios for multiple RLE pairs (Figs. B.3 and 4). Their RLE ratios are not clearly related to their petrological types (e.g., PP, PO, POP). The most significant ones are ratios of Nb to other RLE, with average Nb/Ta (13.4 ± 1.6 , $2\sigma_m$) and Nb/La (0.691 ± 0.131 , $2\sigma_m$) being $\sim 30\%$ and $\sim 40\%$ lower than the CI ratios (~ 19 and ~ 1.1 ; Münker et al., 2003; Barrat et al., 2012; Braukmüller et al., 2018; Lodders, 2020), respectively. EC chondrules, on average, also show lower Zr/Hf (30.0 ± 1.5 , $2\sigma_m$), Sm/Nd (0.281 ± 0.021 , $2\sigma_m$) and Ca/Al (0.848 ± 0.061 , $2\sigma_m$) values, and elevated Al/Ti (33.3 ± 3.1 , $2\sigma_m$) as compared to the CI values (i.e., -12% , -15% , -20% and $+75\%$ relative to CI, respectively). On the other hand, an average ratio of Y and its geochemical twin Ho in EC chondrules (25.8 ± 0.7 , $2\sigma_m$) overlaps the CI composition.

It should be noted that the bulk composition of individual chondrules derived by surface analytical methods (i.e., broadened or scanning beam measurements on thin or thick sections) can be less accurate than those determined by a whole-rock measurement of mechanically separated chondrules (see Section B.2). Our data for Nb/La , Zr/Hf , Al/Ti , and Ca/Al in EC chondrules are consistent with EH4 chondrule compositions from Gerber (2012), who measured elemental abun-

dances of solutions of mechanically isolated individual chondrules using ICP-MS and ICP-OES techniques. Slightly elevated Y/Ho and Sm/Nd ratios of EH4 chondrules from Gerber (2012) might reflect distinct behavior of these elemental twins during thermal processing in the EC parent bodies (Barrat et al., 2014). We consider this consistency as reflecting representative sampling of the bulk EC chondrule compositions in our measurements. Furthermore, our bulk EC chondrule data are generally consistent with results from previous studies which used surface analytical methods (Grossman et al., 1985; Schneider et al., 2002; Varela et al., 2015). Further discussions on the comparison of data obtained in this and previous studies are provided in Section B.2.

3.2 Sulfides from unequilibrated enstatite chondrites

Both EH3 and EL3 chondrites contain abundant opaque nodules with variable mineralogies. They are commonly composed of Si-bearing Fe-Ni metal and troilite, with minor occurrence of exotic sulfides including oldhamite, daubréelite ($\text{Fe}^{2+}\text{Cr}_2^{3+}\text{S}_4$), niningerite (in EH3), alabandite (in EL3), K-bearing sulfides, and phosphides. We report only trace element abundances of EC sulfides which occur outside of EC chondrules, as those found within chondrules are tiny (mostly $< 10 \mu\text{m}$), making analysis by LA-ICP-MS impractical.

Troilites from the primitive EC contain RLE such as Ti (2–7 \times CI), Nb (mostly 0.1–5 \times CI) and Zr (up to 0.2 \times CI), along with nominally chalcophile Cr, Mn and V (Fig. 5; see also Section B.3). In contrast, Ta and Hf, which are geochemical twins of Nb and Zr, respectively, were not detected in the EC troilites. Oldhamites in EC are enriched in multiple RLE, including Zr, Hf, Y, REE, Th and U (Fig. B.4). Most oldhamites show nearly flat REE pattern at 10–100 times higher concentrations than CI, with slightly positive Eu and Yb anomalies in those from EH. They show Zr/Hf (40–600) higher than CI, and variable Sm/Nd (0.34 ± 0.11 , $2\sigma_m$), Y/Ho (31 ± 7 , $2\sigma_m$) and Th/U (4.5 ± 2.5 , $2\sigma_m$) values, which are generally consistent with data reported in Gannoun

et al. (2011). Niningerites in EH are enriched in Sc ($2\text{--}12 \times \text{CI}$) and Zr ($0.2\text{--}16 \times \text{CI}$) (Table E.3). Aluminum was not detected in nearly all of sulfide measurements, indicating that it retains its lithophile behavior under highly reducing conditions.

3.3 Refractory inclusions from unequilibrated carbonaceous chondrites

CAI and AOA from CV chondrites show highly fractionated RLE compositions (Figs. B.5 and B.6; see also Section B.4), reflecting the volatility-driven fractionation of RLE during condensation of these inclusions (e.g., Boynton, 1975). Their RLE compositions are generally consistent with previous studies (e.g., Boynton, 1975; Mason and Martin, 1977; Kornacki and Fegley, 1986; Stracke et al., 2012; Patzer et al., 2018 and references therein). CAI and spinel-rich AOA show low Nb/Ta ratios (3–10), whereas olivine-rich AOA show higher values (18–37). The CV CAI and AOA also show fractionated Zr/Hf (mostly 33–55), Y/Ho (17–38), and Sm/Nd (0.12–0.54) values.

4 Discussion

4.1 RLE fractionation under reduced conditions

Ratios of RLE in individual chondrules from EC, OC, and CC can provide useful insights into distribution and fractionation processes of RLE in the accretionary disk. Although chondrules show considerable scatter in RLE ratios (Fig. 4), their mean compositions provide a measure of distinction between each chondrite class (EC, OC, and CC), reflecting limited mixing of distinct chondrule reservoirs (e.g., Clayton, 2003; Hezel and Parteli, 2018). Here we propose that RLE fractionation processes recorded in highly reduced EC chondrules are distinct from those in less reduced OC and CC chondrules.

It is well recognized and demonstrated that an incomplete high-temperature condensation from

the gas of solar composition can fractionate RLE, as recorded in CAI and AOA (Fig. B.5; e.g., Boynton, 1975; Kornacki and Fegley, 1986; Ruzicka et al., 2012). Nb/Ta ratios of all studied CAI and Ca, Al-rich AOA range from 3 to 10 (Fig. B.6), which are clearly lower than the CI value. In contrast, olivine-rich, less refractory AOA do not show such low Nb/Ta ratios. The low Nb/Ta ratios observed in CAI and refractory-rich AOA might reflect Nb-Ta fractionation during formation of high-temperature nebular condensates, due to slightly different condensation temperatures of these geochemical twins (1559 K and 1573 K for Nb and Ta, respectively) (Lodders, 2003; Münker et al., 2003). Similarly, a slightly higher 50% condensation temperatures of Zr and Y compared to their geochemical twins Hf and Ho, respectively, can produce condensates with non-CI Zr/Hf and Y/Ho ratios (Figs. B.5 and B.6B,E; El Goresy et al., 2002; Pack et al., 2007; Patzer et al., 2010, 2018; Stracke et al., 2012). The non-CI Nb/Ta, Zr/Hf and Y/Ho values in bulk OC and CC chondrites have been attributed to additions of the refractory materials with fractionated RLE compositions into OC and CC asteroids (Münker et al., 2003; Pack et al., 2007; Patzer et al., 2010; Stracke et al., 2012). Likewise, these additions might also be responsible for chondrules possessing similar fractionated Nb/Ta and Zr/Hf ratios (e.g., Misawa and Nakamura, 1988a,b; Pack et al., 2004; Patzer et al., 2018). In contrast, the CI-like average Y/Ho in OC and CC chondrules indicate a similar behavior of these geochemical twins during formation of these chondrules and their precursors (Pack et al., 2007).

Compared to OC and CC chondrules, EC chondrules show more distinct differences in key RLE ratios (e.g., Nb/Ta, Nb/La, Zr/Hf, Sm/Nd, Al/Ti, Ca/Al; Figs. 4 and B.3). Importantly, most RLE are depleted relative to Al in EC chondrules (e.g., super-CI Al/Ti and sub-CI Ca/Al); this feature is distinct from CI-like RLE/Al values in OC and CC chondrules (Figs. 2 to 4). These differences indicate that RLE fractionation processes recorded in EC chondrules differ from those of OC and CC chondrules (i.e., volatility-driven fractionation; Misawa and Nakamura, 1988a,b; Pack et al., 2004; Patzer et al., 2018).

The fractionated RLE ratios in EC chondrules might indicate depletion of moderately chal-

cophile elements under highly reducing conditions (e.g., Ca, REE, Ti, Nb, Zr; Figs. 5 and B.4; Gannoun et al., 2011; Barrat et al., 2014; Lehner et al., 2014) due to separation of sulfides from silicates. The high Al/Ti and low Nb/Ta and Zr/Hf in EC chondrules are consistent with separation of Ti, Nb, Zr-bearing troilites from a precursor with CI composition. The sub-CI Ca/Al and REE/Al in EC chondrules are in harmony with a removal of REE-bearing oldhamite. The separation of oldhamites can also produce sub-CI Sm/Nd and negative Eu and Yb anomalies of EC chondrules (Figs. 2 to 4), given high Sm/Nd and positive Eu and Yb anomalies in oldhamites (Fig. B.4; Gannoun et al., 2011; Jacquet et al., 2015). In addition, smaller depletions of Hf and Ta as compared to their geochemical twins Zr and Nb, respectively (Figs. 2 and 3), indicate the former's more lithophile behavior (Barrat et al., 2014; Münker et al., 2017). Furthermore, The CI-like Y/Ho values of EC chondrules are consistent with limited fractionation of Y/Ho in EC oldhamites (31.3 ± 6.7 , $2\sigma_m$; Table A.3) from the CI ratio (~26; Pack et al., 2007; Barrat et al., 2012; Lodders, 2020). The stronger depletion of the troilite-loving elements (e.g., Ti, Nb) compared to the oldhamite-loving ones' (e.g., REE, Y) in EC chondrules documents a greater contribution of troilite separation to their fractionated RLE compositions. This observation is consistent with a simple mass-balance consideration of modal abundances of sulfides in type 3 EC (Weisberg and Kimura, 2012) and their average RLE concentrations (this study; Gannoun et al., 2011) that indicate the separation of RLE-bearing troilites produces >2 times larger RLE fractionation in residual silicates than the removal of oldhamite.

Chondrules from all types of chondrites are depleted in normally siderophile and chalcophile elements, due to a separation of metal and sulfide components from silicates before and/or during chondrule formation (Osborn et al., 1973; Gooding et al., 1980; Grossman et al., 1985; Palme et al., 2014). For example, it is suggested that metals and sulfides can be expelled from silicate melt droplets during the chondrule formation as immiscible melts (Rambaldi and Wasson, 1981, 1984; Grossman and Wasson, 1985; Zanda et al., 1994; McCoy et al., 1999; Connolly et al., 2001; Uesugi

et al., 2008). In addition, if metal/sulfide and silicate occurred separately in the protoplanetary disk as a result of the chondrule formation and/or nebular condensation, they could have been physically sorted due to their distinct density, size, magnetism, and/or thermal conductivity (Kuebler et al., 1999; Wurm et al., 2013; Kruss and Wurm, 2020; Palme et al., 2014). These separation processes can also contribute to the chalcophility-dependent fractionation of elements in EC chondrules.

The origin of metal-sulfide nodules in EC remains controversial. One view is that they are highly reduced nebular condensates formed and processed separately from silicates before planetesimal formation (Larimer, 1975; Larimer and Bartholomay, 1979; Larimer and Ganapathy, 1987; El Goresy et al., 1988; Kimura, 1988; Lin and El Goresy, 2002; Gannoun et al., 2011; El Goresy et al., 2017), whereas others propose that they were ejected from chondrule-forming melt droplets as immiscible liquids (Hsu, 1998; Horstmann et al., 2014; Lehner et al., 2014; Ebel et al., 2015; Jacquet et al., 2015; Piani et al., 2016) or combination of these processes (Lehner et al., 2010). The post-accretionary impact origin of these nodules is inconsistent with a lack of petrological and chemical features of in-situ melting (Horstmann et al., 2014; Gannoun et al., 2011; El Goresy et al., 2017).

The formation of metal-sulfide nodules and their separation from silicates can be critical processes in establishing Fe/Si ratio of bulk bodies with highly reduced oxidation states. The lower bulk Fe/Si value of EL chondrites as compared to EH (Fig. 1) can be partly attributed to less abundant occurrence of troilite in EL (<8 vol% and >10 vol% in primitive EL and EH, respectively; Weisberg and Kimura, 2012). If the low troilite abundance in EL reflect the ejection of sulfides from chondrule-forming silicate melts and their limited accretion to the EL parent bodies, the bulk EL should be depleted in moderately chalcophile RLE. However, neither bulk EH3 nor EL3 shows fractionated RLE compositions (Barrat et al., 2014). Even ratios of RLE with different chalcophile affinities (e.g., Nb/La, Zr/Hf, Sc/Hf, Sc/Nb) are CI-like in the bulk EC (Barrat et al., 2014), which are distinct from highly fractionated RLE compositions of their chondrules (Figs. 2 to 4). These ob-

servations suggest that the depletion of moderately chalcophile RLE in EC silicates (i.e., chondrules) are fully compensated by the occurrence of RLE-bearing sulfides in the bulk EC, and removal of sulfides from chondrule-forming melts did not contribute to the low troilite abundance in EL. Thus, the metal- and sulfide-depletion in EC chondrules and the CI-like RLE ratios of the bulk EC indicate that EC silicates and metal-sulfide nodules occurred as separate objects in the protoplanetary disk, but none of them was preferentially removed from the reservoir before and during the EC parent body accretion. The limited physical sorting of the EC silicates, sulfides, and metals indicates that their separation was a localized process in the protoplanetary disk, and EC parent bodies accreted quickly after the chondrule formation events. The fractionated RLE ratios of EC components (Fig. 4) and solar-like RLE ratio of the bulk EC (Barrat et al., 2014) might support a compositional complementarity between chondrules and other components (e.g., Hezel et al., 2018).

In order to further constrain the timing and mechanism of RLE fractionation recorded by EC chondrules and sulfides, especially those in EH, it demands an understanding of the redox-dependent changes of RLE volatilities. Although multiple equilibrium condensation calculations have been performed for highly reducing conditions (e.g., Larimer, 1975; Larimer and Bartholomay, 1979; Lodders and Fegley, 1993; Wood and Hashimoto, 1993; Sharp and Wasserburg, 1995; Ebel, 2006; Ebel and Alexander, 2011), relative volatilities of minor and trace RLE, especially those for troilite-loving ones (e.g., Ti, Nb), are poorly constrained. A combination of relative volatilities and chalcophile affinities of RLE under reducing conditions will provide important constraints on the RLE fractionation mechanism prior to the accretion of EC parent bodies.

4.2 Compositional difference between EC chondrules and the silicate Earth

The limited variation (<10%) in RLE ratios among chondritic meteorites and the solar photosphere have led planetary scientists to use the constant RLE ratio rule in their compositional models of planets (Section 1). In contrast, the fractionated RLE ratios of EC chondrules (Figs. 2 to 4) potentially

places limits on the use of this rule, when modeling composition of highly reduced bodies (e.g., Mercury; Section 4.4). In turn, these variations can be used as a new key to reveal the nature of planetary building blocks, together with the isotopic constraints (e.g., Javoy et al., 2010; Warren, 2011; Dauphas, 2017).

Isotopic similarities of Earth and EC suggest EC-like materials as the Earth's main building block (e.g., Javoy et al., 2010; Warren, 2011; Dauphas, 2017; Boyet et al., 2018). In this case, the Earth's mantle could have been dominated by EC chondrule-like materials, as they host nearly all of silicates in EC (e.g., Weisberg and Kimura, 2012; Krot et al., 2014). EC chondrules and the Earth's mantle share Nb depletions, with Nb/Ta and Nb/La values being 20–30% lower than the CI chondritic values (Fig. 4; Münker et al., 2003). In contrast, composition of terrestrial komatiites, high-temperature ultramafic rocks mostly formed in the Archean, is consistent with a CI-like Ti/RLE values for the Earth's primitive mantle, and thus there is no Ti depletion in the BSE (e.g., Nesbitt et al., 1979; McDonough and Sun, 1995; Arndt, 2003). The fractionated Al/Ti values of EC chondrules highlight their compositional distinction from the BSE.

Experimental studies show that Nb and Ti have similar $D^{\text{sulfide}/\text{silicate}}$ values at wide P , T , and f_{O_2} conditions, with the value exceeding 1 at highly reduced conditions ($\log f_{\text{O}_2} \leq \text{IW} - 2$; Fig. 6A; Kiseeva and Wood, 2015; Wood and Kiseeva, 2015; Namur et al., 2016; Münker et al., 2017; Cartier et al., 2020; Steenstra and van Westrenen, 2020). Compositions of troilites and silicates from aubrites, highly reduced achondrites, support similar chalcophilicities of Nb and Ti during differentiation of aubrite parent bodies (van Acken et al., 2012; Münker et al., 2017). These observations suggest that a sulfide-silicate fractionation under highly reduced conditions produces not only Nb, but also Ti depletion in silicates at a similar degree. However, unlike Nb, Ti is not depleted in the BSE (e.g., Nesbitt et al., 1979; McDonough and Sun, 1995; Arndt, 2003). Thus, even if the EC chondrules are the Earth's main building block (Javoy et al., 2010; Warren, 2011; Dauphas, 2017; Boyet et al., 2018), the accessible Earth's Nb depletion should not have resulted

from a sulfide-silicate separation under highly reduced conditions. The negligible role of highly reduced sulfide in the present-day Earth’s composition is also consistent with CI-like REE abundance of the BSE (e.g., McDonough and Sun, 1995; Pack et al., 2007; Bouvier et al., 2008; Bouvier and Boyet, 2016; Burkhardt et al., 2016) (cf. Stracke et al., 2012; Dauphas and Pourmand, 2015) and a lack of evidence for Th and U incorporation into the Earth’s core (Wipperfurth et al., 2018).

The relative partitioning behaviors of Nb and Ti are also useful when considering a compositional evolution of the Earth’s mantle. Sub-CI Nb/RLE and CI-like Ti/RLE ratios of komatiites and Archean basalts indicate the Nb depletion in the silicate mantle was produced before the Archean, with negligible Ti depletion (Nesbitt et al., 1979; Arndt, 2003; Münker et al., 2003). This observation cannot easily be accommodated with the formation of refractory rutile-bearing hidden eclogite reservoir (Rudnick et al., 2000; Kamber and Collerson, 2000; Nebel et al., 2010), which might produce both Nb and Ti depletion in the accessible Earth (Schmidt et al., 2004).

Experimental studies show that Nb becomes siderophile under reducing conditions ($\log f_{\text{O}_2} \leq \text{IW} - 2$), whereas Ti remains lithophile (Fig. 6B; Wade and Wood, 2001; Corgne et al., 2008; Mann et al., 2009; Namur et al., 2016; Cartier et al., 2020; Steenstra and van Westrenen, 2020). Thus, a metal-silicate differentiation under reduced conditions can selectively separate Nb from silicate melts, and leave Ti as oxide in the mantle. Therefore, the siderophile behavior of Nb under reduced conditions might be a most plausible scenario for the origin of the BSE’s Nb depletion (Wade and Wood, 2001; Münker et al., 2003). Recently, Münker et al. (2017) experimentally showed that Nb becomes less chalcophile when Fe/S of a sulfide melt increases. Thus, it is likely that the siderophile behavior of Nb in the Earth reflects the low S content of the Earth’s core (Dreibus and Palme, 1996; McDonough, 2014).

4.3 The Earth's building blocks

The fractionated RLE ratios in EC components provide insights into the nature of the Earth's building blocks, which are considered to be dominated by EC-like materials based on isotopic constraints (e.g., Javoy et al., 2010; Warren, 2011; Dauphas, 2017; Boyet et al., 2018). Multiple observations suggest that the BSE has CI-like RLE ratios (e.g., Al/Ti, Zr/Hf, Ca/Al and Sm/Nd, excepting possibly Nb/RLE; McDonough and Sun, 1995; Münker et al., 2003; Stracke et al., 2012; Bouvier et al., 2008; Bouvier and Boyet, 2016; Burkhardt et al., 2016; Willig and Stracke, 2019; Hasenstab et al., 2020). If the Earth's accretion was dominated by highly reduced, EC-like materials, their silicate fraction might have fractionated RLE ratios due to depletion of nominally lithophile, but moderately chalcophile refractory elements (e.g., Ti, Zr, Ca, REE), as we have observed in EC chondrules (Figs. 2-4). To produce the CI-like RLE ratios of the BSE, the reduced silicates and RLE-bearing sulfides should have been jointly incorporated into the accreting Earth. Subsequently, RLE hosted in these sulfides from the impactors must have been re-incorporated into the silicate mantle, which is consistent with a progressive oxidation of the Earth's interior (Corgne et al., 2008; Mann et al., 2009; Schönbächler et al., 2010; Rubie et al., 2011, 2015). An important implication of this scenario is that the Earth's silicates and sulfides should have originated in the same chemical reservoir which originally had a solar-like unfractionated RLE composition. In addition, these silicates and sulfides should have accreted to planetesimals before being physically separated in the protoplanetary disk.

Alternatively, the distinct RLE composition of silicate fractions of EC and Earth might reflect distinct formation temperatures of their precursors. Importantly, the bulk Earth is depleted in S, but have chondritic Fe/Si value (Dreibus and Palme, 1996; McDonough, 2014), indicating that its S depletion was established during a nebular condensation, rather than separation of sulfides from silicates by the physical sorting within the accretionary disk. Under highly reducing nebular conditions as recorded by EC, refractory sulfides such as oldhamite and niningerite condense at 1000–800

K, whereas troilite condenses at <700 K as a major S-bearing phase (Hutson and Ruzicka, 2000; Pasek et al., 2005). Therefore, RLE compositions of highly reduced silicates condensed before the condensation of these sulfides should not have been fractionated due to sulfide-silicate separation as recorded in EC chondrules. This scenario supports the condensation of Earth's precursors at higher temperatures as compared to the EC materials, which have been previously proposed based on the EC's elevated abundances of moderately volatile elements and low Mg/Si and RLE/Mg ratios of EC (Kerridge, 1979; Larimer, 1979; Dauphas et al., 2015; Morbidelli et al., 2020; Yoshizaki and McDonough, 2021).

Our observations revealed distinct RLE compositions of the silicate fractions of EC and Earth, which further emphasize their compositional distinctions (Palme et al., 1988; McDonough and Sun, 1995; Yoshizaki and McDonough, 2021). The distinction between EC and Earth reflects an unrepresentative sampling of the solar system materials in our meteorite collections due to restricted source regions of meteoritic samples (DeMeo and Carry, 2014; Heck et al., 2017) and/or a lack of leftovers of the Earth's building blocks in the present-day solar system (Drake and Righter, 2002). Although there is no meteorite group that matches the chemical and isotopic composition of Earth, EC and their components provide unique and useful guides to the origin, nature, and geochemical evolution of the Earth-forming materials (Dauphas et al., 2015; Morbidelli et al., 2020; Yoshizaki and McDonough, 2021).

4.4 Implications for the composition of Mercury

The RLE fractionation observed in the silicate fraction of EC (Figs. 2 to 4) indicates that caution is needed when modeling RLE abundance of highly reduced bodies that have experienced an open-system metal-silicate separation (e.g., physical sorting before and during planetary accretion, collisional erosion of a mantle). The most notable example is Mercury, which is one of the most reduced bodies in our solar system and has an elevated bulk Fe/Si ratio that might reflect a selective

removal of silicates and/or preferred accretion of metal/sulfide phases (Nittler et al., 2011; Ebel and Stewart, 2018; Margot et al., 2018).

The elemental abundance of the Mercury's surface was measured by the MErcury Surface, Space ENvironment, GEochemistry, and Ranging (MESSENGER) spacecraft, which provided important constraints on the chemical composition and interior structure of the planet (Nittler et al., 2011, 2018, 2020; Peplowski et al., 2011). Recently, Cartier et al. (2020) showed that Al/Ti ratio in the bulk silicate Mercury is \sim 50% higher than the CI value, based on the MESSENGER data. By assuming that the bulk Mercury has a chondritic Al/Ti value, the authors concluded that the Ti depletion in the Mercury's surface was produced by a S-bearing core formation under reducing condition, and estimated a thickness of a troilite layer at the core-mantle boundary. In contrast, chondrules and sulfides from EC show clear evidence for Al/Ti fractionation in a highly reduced nebular environment before planetary accretion and differentiation (Fig. 4). Therefore, the super-CI Al/Ti value of the Mercury's silicate shell might reflect both nebular and planetary RLE fractionation processes under reducing conditions. Importantly, if the planet preferentially accreted metal/sulfide phases (Wurm et al., 2013; Kruss and Wurm, 2018, 2020), bulk Mercury can be enriched in moderately chalcophile RLE (e.g., Ti, REE, Nb, Ca) compared to Al, thereby invalidating the constant RLE ratio rule. Thus, the constant RLE rule should be used with caution, at least when estimating chemical compositions of highly reduced bodies.

As we described in Section 4.3, highly reduced silicates condensing from a cooling nebular gas before the condensation of RLE-bearing sulfides may not be affected by a significant RLE fractionation due to sulfide-silicate separation. The observations by the MESSENGER mission indicate that the surface materials of Mercury have less fractionated RLE ratios and lower abundances of moderately volatile elements as compared to the silicate fractions of EC (Nittler et al., 2011, 2018, 2020; Peplowski et al., 2011; Evans et al., 2015; Cartier et al., 2020). These observations might suggest that the building blocks of Mercury have condensed at higher temperatures than EC materials (i.e.,

before sulfide condensation), as we proposed for the Earth’s precursor materials.

5 Conclusions

Refractory lithophile elements (RLE) can be fractionated due to their different chalcophile affinities under highly reducing nebular conditions. Chondrules from enstatite chondrites (EC) record RLE fractionation due to a sulfide-silicate separation before and/or during chondrule formation events under a highly reduced nebular environments, documenting that RLE ratios can be variable among silicates in the planetary building blocks. In contrast, the bulk EC have CI-like RLE ratios, indicating a negligible physical sorting of silicates and sulfides before and during the accretion of EC parent bodies. Similarly, the Earth’s building blocks might have not experienced the physical sorting of silicates and sulfides. Alternatively, they have condensed from a high-temperature nebular gas in which RLE-bearing sulfides were not stable. The accessible Earth’s Nb depletion and its chondritic Ti/RLE values might reflect the moderately siderophile behavior of Nb during the Earth’s accretion. The moderately chalcophile behavior of RLE under highly reducing conditions indicate that the bulk Mercury cannot yield CI-like RLE ratios if its large core/mantle ratio is originated in a selective removal of silicates.

Acknowledgments

We thank Roberta Rudnick and Philip Piccoli for discussions and technical assistance, Issei Narita for technical assistance, Dominik Hezel for kindly providing the ChondriteDB spreadsheet. We appreciate Conel Alexander and Kevin Righter for their helpful comments. We greatly appreciate Herbert Palme, Andreas Stracke, Dominik Hezel, and an anonymous referee for their constructive reviews, which helped improve the manuscript. We thank the associate editor Stefan Weyer for his editorial effort. We are grateful to NASA/JSC for loan of ALH 84170, ALH 84206, ALH 85119,

MAC 88136 and RBT 04143, National Institute of Polar Research for ALHA77295, and the Smithsonian Institute for Allende. This work was supported by Grant-in-Aid for JSPS Research Fellow (No. JP18J20708), GP-EES Research Grant and DIARE Research Grant to TaY, JSPS KAKENHI Grant (No. 16H04081) to TeY, and NSF grant EAR1650365 to WFM.

Author contributions

Takashi Yoshizaki: Conceptualization, Methodology, Validation, Formal analysis, Investigation, Resources, Data Curation, Writing—Original Draft, Visualization, Project administration, Funding acquisition. **Richard D. Ash:** Methodology, Validation, Formal analysis, Investigation, Writing—Review & Editing. **Marc D. Lipella:** Formal analysis, Investigation, Data Curation. **Tetsuya Yokoyama:** Writing—Review & Editing, Funding acquisition. **William F. McDonough:** Conceptualization, Methodology, Validation, Formal analysis, Writing—Review & Editing, Funding acquisition.

Competing financial interests

The authors declare no competing financial interests.

Supplementary materials

Supplementary materials associated with this article can be found in the online version.

Table 1: List of meteorite samples used in this study. Meteorite types and weathering grades are based on the online Meteoritical Bulletin Database (www.lpi.usra.edu/meteor/) and Satterwhite and Righter (2007). Abbreviations: NIPR–National Institute of Polar Research; SI–Smithsonian Institution.

Name	Type	Weathering grade	Sample source
ALHA77295	EH3	B	NIPR
ALH 84206	EH3	A/B	NASA/JSC
ALH 84170	EH3	B	NASA/JSC
MAC 88136	EL3	A	NASA/JSC
ALH 85119	EL3	Be	NASA/JSC
RBT 04143	CV3	B	NASA/JSC
Allende	CV3	Fall	SI

Table 2: Conditions of the LA-ICP-MS measurement.

Thermo Finnigan Element2 single-collector, sector field ICP-MS

Forward power	1265 W
HV	8 kV
Number of pre-scans	1
Active dead time	18 ns
Cool gas flow	16 L/min Ar
Auxiliary gas flow	1.05 L/min Ar
Sample gas flow	1.040 L/min Ar
Autosampler	ASX-100 (CETAC Technologies)
Torch	Quartz
Injector	Quartz
Skimmer cone	Al-alloy
Sampling cone	Al-alloy
Detection mode	Analogue or both
Dwell time	20 s background acquisition, 40 s data acquisition
Samples/peak	1
Runs*passes	100*1
Search window	150%
Integration window	80%
Integration type	Intensities
Scan type	EScan
Oxide forming rate	$^{238}\text{U}^{16}\text{O}/^{238}\text{U} < 2.0\%$

Electro Scientific New Wave frequency-quintupled Nd:YAG laser (213 nm) system

Ablation pattern	Spot
Spot diameter	15–200 μm
Repetition rate	7 Hz
Energy density	2–3 J/cm ²

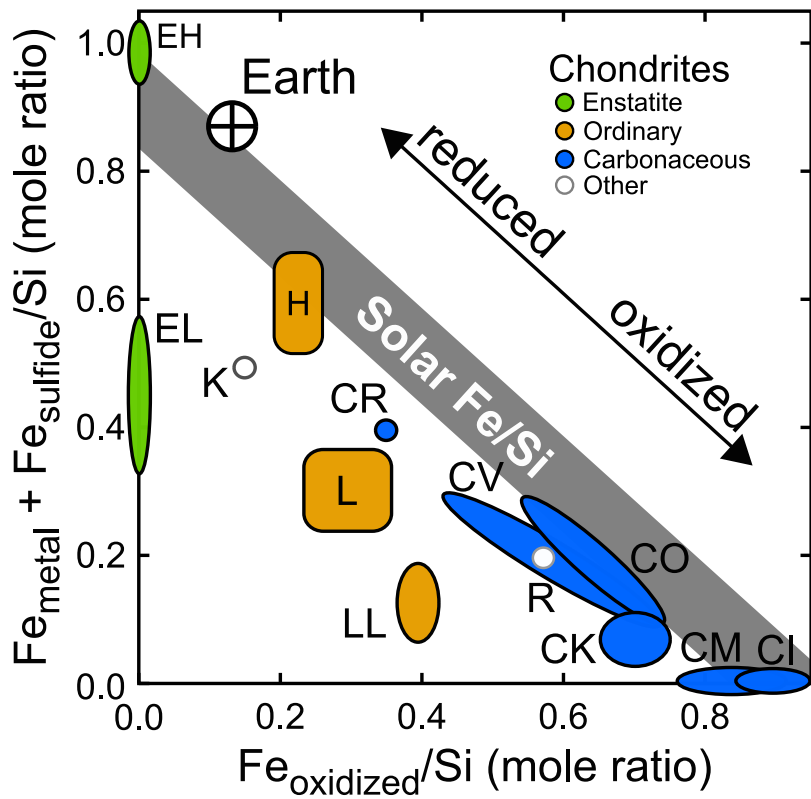


Fig. 1: The Urey-Craig diagram showing variation in oxidation state of iron relative to silicon among chondrite groups (after Urey and Craig, 1953). The plot of Earth is based on McDonough (2014). Metal-rich CB and CH chondrites are not included in the plot because their origin (condensation from a gas-melt plume formed by a planetary-scale collision; e.g., Krot et al., 2012) is distinct from that of major chondrite groups.

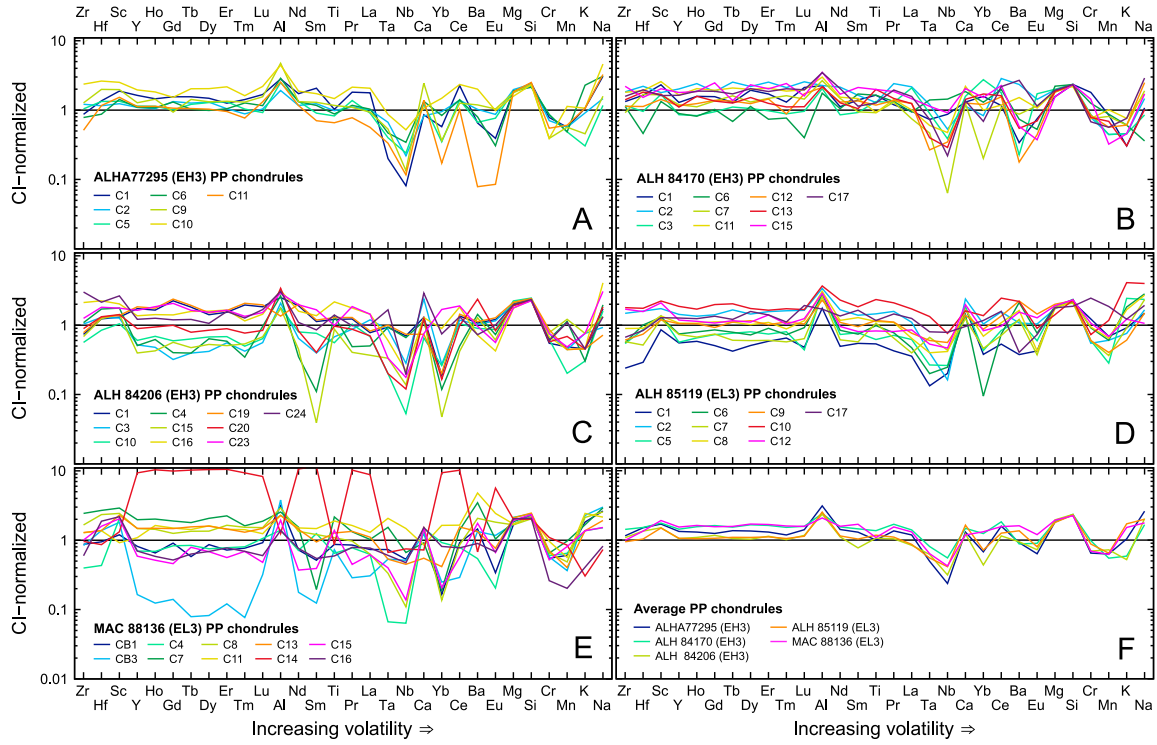


Fig. 2: (A–E) CI-normalized (Lodders, 2020) abundances of lithophile elements in selected porphyritic pyroxene (PP) chondrules from unequilibrated enstatite chondrites, and (F) average composition of PP chondrules in each sample.

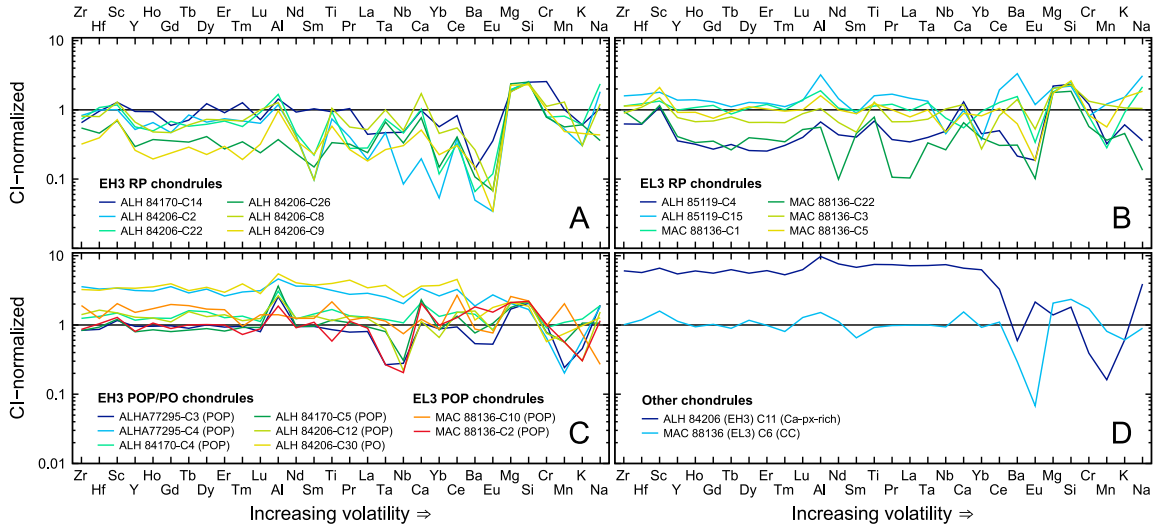


Fig. 3: CI-normalized (Lodders, 2020) abundances of lithophile elements in non-PP chondrules from unequilibrated enstatite chondrites. Abbreviations: CC—cryptocrystalline; PO—porphyritic olivine; POP—porphyritic olivine pyroxene; RP—radial pyroxene.

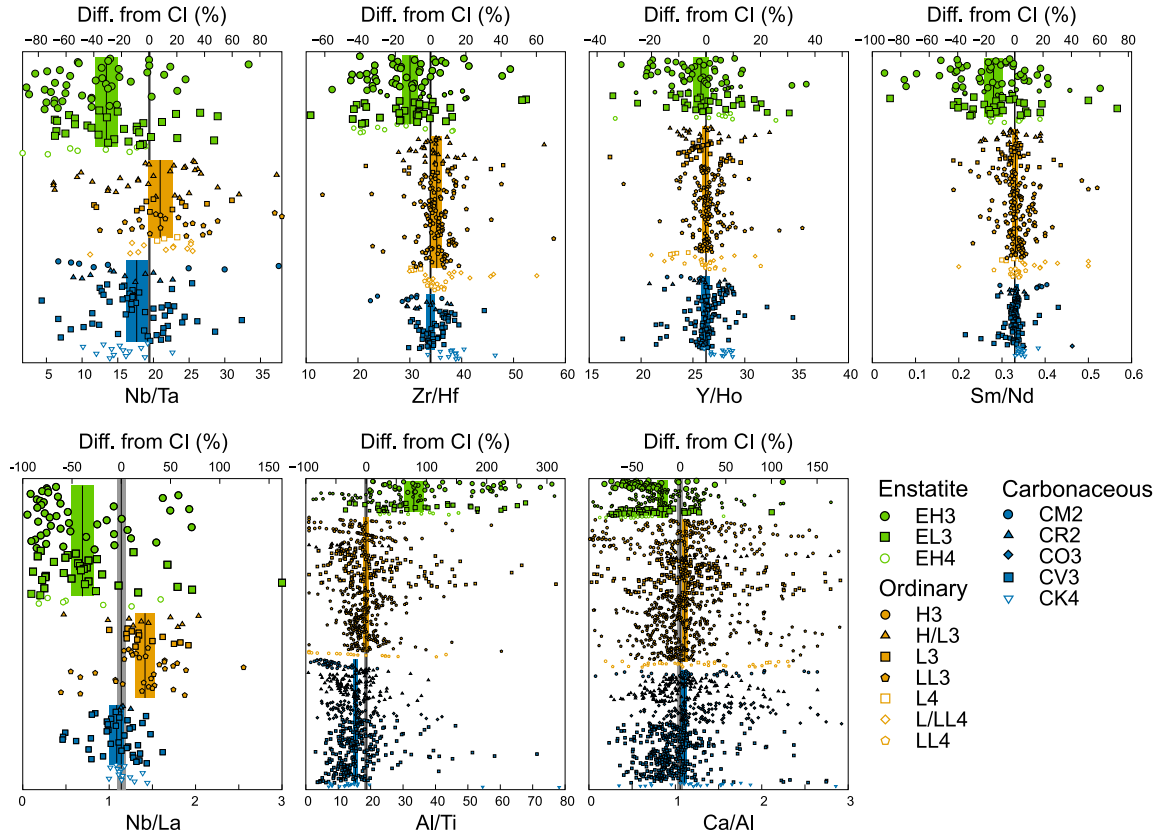


Fig. 4: Refractory lithophile element ratios (Nb/Ta, Zr/Hf, Y/Ho, Sm/Nd, Nb/La, Al/Ti, and Ca/Al) of bulk chondrules from unequilibrated type 3 enstatite (green), ordinary (orange) and carbonaceous (blue) chondrites. Our new data for type 3 EC chondrules are shown by large filled green circles (EH3) or squares (EL3). Colored boxes and inside solid lines represent mean $\pm 2\sigma_m$ values for each chondrite groups. Gray box and inside solid line correspond mean $\pm 2\sigma_m$ for CI chondrite (Barrat et al., 2012; Lodders, 2020). Data for chondrules from metamorphosed type 4 samples are also shown for a comparison. Most literature data are obtained from the ChondriteDB Database (Hezel et al., 2018b). A list of full data sources is provided as a supplementary material.

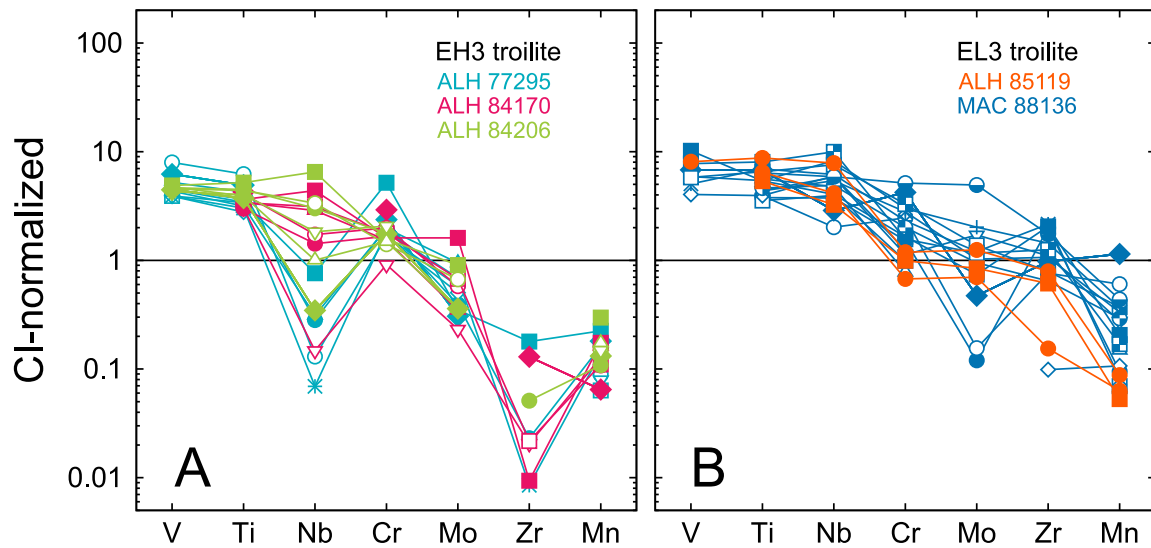


Fig. 5: Transition element composition of troilites (FeS) from unequilibrated EH and EL chondrite, normalized to CI chondrite composition (Lodders, 2020).

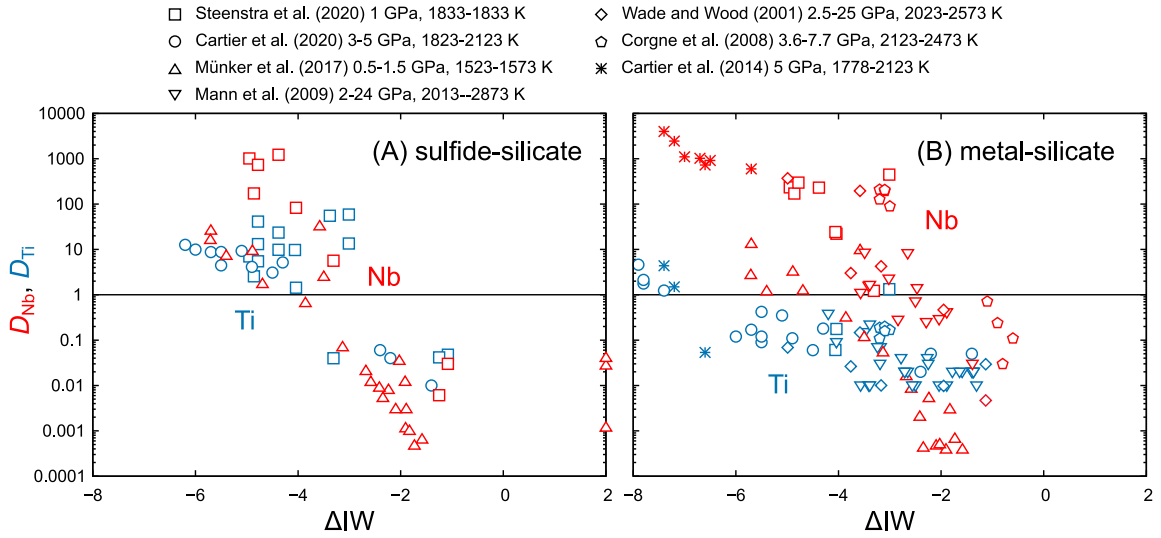


Fig. 6: (A) Sulfide-silicate and (B) metal-silicate partition coefficients of Nb (blue) and Ti (red) reported by previous studies (Wade and Wood, 2001; Corgne et al., 2008; Mann et al., 2009; Cartier et al., 2014, 2020; Münker et al., 2017; Steenstra and van Westrenen, 2020).

References

- van Achterbergh, E., Ryan, C.G., Jackson, S.E., Griffin, W.L., 2001. Appendix 3: Data reduction software for LA-ICP-MS, in: Sylvester, P. (Ed.), *Laser Ablation-ICP-MS in the Earth Sciences: Principles and Applications*. Mineralogical Association of Canada, Québec. volume 29 of *Mineralogical Association of Canada—Short Course Series*, pp. 239–243.
- van Acken, D., Humayun, M., Brandon, A.D., Peslier, A.H., 2012. Siderophile trace elements in metals and sulfides in enstatite achondrites record planetary differentiation in an enstatite chondritic parent body. *Geochimica et Cosmochimica Acta* 83, 272–291. doi:10.1016/j.gca.2011.12.025.
- Alexander, C.M.O., 2005. Re-examining the role of chondrules in producing the elemental fractionations in chondrites. *Meteoritics & Planetary Science* 40, 943–965. doi:10.1111/j.1945-5100.2005.tb00166.x.
- Alexander, C.M.O., 2019a. Quantitative models for the elemental and isotopic fractionations in chondrites: The carbonaceous chondrites. *Geochimica et Cosmochimica Acta* 254, 277–309. doi:10.1016/j.gca.2019.02.008.
- Alexander, C.M.O., 2019b. Quantitative models for the elemental and isotopic fractionations in the chondrites: The non-carbonaceous chondrites. *Geochimica et Cosmochimica Acta* 254, 246–276. doi:10.1016/j.gca.2019.01.026.
- Allègre, C.J., Poirier, J.P., Humler, E., Hofmann, A.W., 1995. The chemical composition of the Earth. *Earth and Planetary Science Letters* 134, 515–526. doi:10.1016/0012-821X(95)00123-T.
- Amsellem, E., Moynier, F., Pringle, E.A., Bouvier, A., Chen, H., Day, J.M.D., 2017. Testing the

chondrule-rich accretion model for planetary embryos using calcium isotopes. *Earth and Planetary Science Letters* 469, 75–83. doi:10.1016/j.epsl.2017.04.022.

Arndt, N.T., 2003. Komatiites, kimberlites, and boninites. *Journal of Geophysical Research: Solid Earth* 108, 2293. doi:10.1029/2002JB002157.

Barrat, J.A., Dauphas, N., Gillet, P., Bollinger, C., Etoubleau, J., Bischoff, A., Yamaguchi, A., 2016. Evidence from Tm anomalies for non-CI refractory lithophile element proportions in terrestrial planets and achondrites. *Geochimica et Cosmochimica Acta* 176, 1–17. doi:10.1016/j.gca.2015.12.004.

Barrat, J.A., Zanda, B., Jambon, A., Bollinger, C., 2014. The lithophile trace elements in enstatite chondrites. *Geochimica et Cosmochimica Acta* 128, 71–94. doi:10.1016/j.gca.2013.11.042.

Barrat, J.A., Zanda, B., Moynier, F., Bollinger, C., Liorzou, C., Bayon, G., 2012. Geochemistry of CI chondrites: Major and trace elements, and Cu and Zn isotopes. *Geochimica et Cosmochimica Acta* 83, 79–92. doi:10.1016/j.gca.2011.12.011.

Benoit, P.H., Akridge, G.A., Ninagawa, K., Sears, D.W.G., 2002. Thermoluminescence sensitivity and thermal history of type 3 ordinary chondrites: Eleven new type 3.0–3.1 chondrites and possible explanations for differences among H, L, and LL chondrites. *Meteoritics & Planetary Science* 37, 793–805. doi:10.1111/j.1945-5100.2002.tb00856.x.

Bonal, L., Gattacceca, J., Garenne, A., Eschrig, J., Rochette, P., Ruggiu, L.K., 2020. Water and heat: New constraints on the evolution of the CV chondrite parent body. *Geochimica et Cosmochimica Acta* 276, 363–383. doi:10.1016/j.gca.2020.03.009.

Bouvier, A., Boyet, M., 2016. Primitive Solar System materials and Earth share a common initial ^{142}Nd abundance. *Nature* 537, 399–402. doi:10.1038/nature19351.

Bouvier, A., Vervoort, J.D., Patchett, P.J., 2008. The Lu–Hf and Sm–Nd isotopic composition of CHUR: Constraints from unequilibrated chondrites and implications for the bulk composition of terrestrial planets. *Earth and Planetary Science Letters* 273, 48–57. doi:10.1016/j.epsl.2008.06.010.

Boyet, M., Bouvier, A., Frossard, P., Hammouda, T., Garçon, M., Gannoun, A., 2018. Enstatite chondrites EL3 as building blocks for the Earth: The debate over the ^{146}Sm – ^{142}Nd systematics. *Earth and Planetary Science Letters* 488, 68–78. doi:10.1016/j.epsl.2018.02.004.

Boynton, W.V., 1975. Fractionation in the solar nebula: Condensation of yttrium and the rare earth elements. *Geochimica et Cosmochimica Acta* 39, 569–584. doi:10.1016/0016-7037(75)90003-4.

Braukmüller, N., Wombacher, F., Hezel, D.C., Escoube, R., Münker, C., 2018. The chemical composition of carbonaceous chondrites: Implications for volatile element depletion, complementarity and alteration. *Geochimica et Cosmochimica Acta* 239, 17–48. doi:10.1016/j.gca.2018.07.023.

Brearley, A.J., Jones, R.H., 1998. Chondritic meteorites, in: Papike, J.J. (Ed.), *Reviews in Mineralogy*. Mineralogical Society of America. volume 36, pp. 3–1–3–398. doi:10.2138/rmg.1999.36.3.

Burkhardt, C., Borg, L.E., Brennecka, G.A., Shollenberger, Q.R., Dauphas, N., Kleine, T., 2016. A nucleosynthetic origin for the Earth's anomalous ^{142}Nd composition. *Nature* 537, 394–398. doi:10.1038/nature18956.

Cartier, C., Hammouda, T., Boyet, M., Bouhid, M.A., Devidal, J.L., 2014. Redox control of the fractionation of niobium and tantalum during planetary accretion and core formation. *Nature Geoscience* 7, 573–576. doi:10.1038/ngeo2195.

- Cartier, C., Namur, O., Nittler, L.R., Weider, S.Z., Crapster-Pregont, E., Vorburger, A., Franck, E.A., Charlier, B., 2020. No FeS layer in Mercury? Evidence from Ti/Al measured by MESSENGER. *Earth and Planetary Science Letters* 534, 116108. doi:10.1016/j.epsl.2020.116108.
- Clayton, R.N., 2003. Oxygen isotopes in meteorites, in: Holland, H.D., Turekian, K.K. (Eds.), *Meteorites, Comets, and Planets*. Elsevier, Oxford. volume 1 of *Treatise on Geochemistry*, pp. 129–142. doi:10.1016/B0-08-043751-6/01063-X.
- Connolly, Jr., H.C., Huss, G.R., Wasserburg, G.J., 2001. On the formation of Fe-Ni metal in Renazzo-like carbonaceous chondrites. *Geochimica et Cosmochimica Acta* 65, 4567–4588. doi:10.1016/S0016-7037(01)00749-9.
- Corgne, A., Keshav, S., Wood, B.J., McDonough, W.F., Fei, Y., 2008. Metal–silicate partitioning and constraints on core composition and oxygen fugacity during Earth accretion. *Geochimica et Cosmochimica Acta* 72, 574–589. doi:10.1016/j.gca.2007.10.006.
- Dauphas, N., 2017. The isotopic nature of the Earth’s accreting material through time. *Nature* 541, 521–524. doi:10.1038/nature20830.
- Dauphas, N., Poitrasson, F., Burkhardt, C., Kobayashi, H., Kurosawa, K., 2015. Planetary and meteoritic Mg/Si and $\delta^{30}\text{Si}$ variations inherited from solar nebula chemistry. *Earth and Planetary Science Letters* 427, 236–248. doi:10.1016/j.epsl.2015.07.008.
- Dauphas, N., Pourmand, A., 2015. Thulium anomalies and rare earth element patterns in meteorites and Earth: Nebular fractionation and the nugget effect. *Geochimica et Cosmochimica Acta* 163, 234–261. doi:10.1016/j.gca.2015.03.037.
- DeMeo, F.E., Carry, B., 2014. Solar System evolution from compositional mapping of the asteroid belt. *Nature* 505, 629–634. doi:10.1038/nature12908.

- Drake, M.J., Righter, K., 2002. Determining the composition of the Earth. *Nature* 416, 39–44. doi:10.1038/416039a.
- Dreibus, G., Palme, H., 1996. Cosmochemical constraints on the sulfur content in the Earth's core. *Geochimica et Cosmochimica Acta* 60, 1125–1130. doi:10.1016/0016-7037(96)00028-2.
- Ebel, D.S., 2006. Condensation of rocky material in astrophysical environments, in: Lauretta, D.S., McSween, Jr., H.Y. (Eds.), *Meteorites and the Early Solar System II*. The University of Arizona Press, Tucson, pp. 253–277.
- Ebel, D.S., Alexander, C.M.O., 2011. Equilibrium condensation from chondritic porous IDP enriched vapor: Implications for Mercury and enstatite chondrite origins. *Planetary and Space Science* 59, 1888–1894. doi:10.1016/j.pss.2011.07.017.
- Ebel, D.S., Boyet, M., Hammouda, T., Gannoun, A., Weisberg, M.K., El Goresy, A., 2015. Complementary rare Earth element abundances in enstatite and oldhamite in EH3 chondrites, in: *Lunar and Planetary Science Conference*, p. 2619.
- Ebel, D.S., Stewart, S.T., 2018. The elusive origin of Mercury, in: Solomon, S.C., Nittler, L.R., Anderson, B.J. (Eds.), *Mercury: The View after MESSENGER*. Cambridge University Press, Cambridge, pp. 497–515. doi:10.1017/9781316650684.019.
- El Goresy, A., Lin, Y., Miyahara, M., Gannoun, A., Boyet, M., Ohtani, E., Gillet, P., Trieloff, M., Simionovici, A., Feng, L., Lemelle, L., 2017. Origin of EL3 chondrites: Evidence for variable C/O ratios during their course of formation—A state of the art scrutiny. *Meteoritics & Planetary Science* 52, 781–806. doi:10.1111/maps.12832.
- El Goresy, A., Yabuki, H., Ehlers, K., Woolum, D., Pernicka, E., 1988. Qingzhen and Yamato-691: A tentative alphabet for the EH chondrites. *Antarctic Meteorite Research* 1, 65–101.

- El Goresy, A., Zinner, E., Matsunami, S., Palme, H., Spettel, B., Lin, Y., Nazarov, M., 2002. Efremovka 101.1: A CAI with ultrarefractory REE patterns and enormous enrichments of Sc, Zr, and Y in fassaite and perovskite. *Geochimica et Cosmochimica Acta* 66, 1459–1491. doi:10.1016/S0016-7037(01)00854-7.
- Evans, L.G., Peplowski, P.N., McCubbin, F.M., McCoy, T.J., Nittler, L.R., Zolotov, M.Y., Ebel, D.S., Lawrence, D.J., Starr, R.D., Weider, S.Z., Solomon, S.C., 2015. Chlorine on the surface of Mercury: MESSENGER gamma-ray measurements and implications for the planet's formation and evolution. *Icarus* 257, 417–427. doi:10.1016/j.icarus.2015.04.039.
- Gannoun, A., Boyet, M., El Goresy, A., Devouard, B., 2011. REE and actinide microdistribution in Sahara 97072 and ALHA77295 EH3 chondrites: A combined cosmochemical and petrologic investigation. *Geochimica et Cosmochimica Acta* 75, 3269–3289. doi:10.1016/j.gca.2011.03.017.
- Gerber, M., 2012. Chondrule formation in the early Solar System: A combined ICP-MS, ICP-OES and petrological study. Ph.D. thesis. University of Münster.
- Gooding, J.L., Keil, K., Fukuoka, T., Schmitt, R.A., 1980. Elemental abundances in chondrules from unequilibrated chondrites: Evidence for chondrule origin by melting of pre-existing materials. *Earth and Planetary Science Letters* 50, 171–180. doi:10.1016/0012-821X(80)90127-2.
- Grossman, J.N., Brearley, A.J., 2005. The onset of metamorphism in ordinary and carbonaceous chondrites. *Meteoritics & Planetary Science* 40, 87–122. doi:10.1111/j.1945-5100.2005.tb00366.x.
- Grossman, J.N., Rubin, A.E., Rambaldi, E.R., Rajan, R.S., Wasson, J.T., 1985. Chondrules in the Qingzhen type-3 enstatite chondrite: Possible precursor components and comparison to ordi-

nary chondrite chondrules. *Geochimica et Cosmochimica Acta* 49, 1781–1795. doi:10.1016/0016-7037(85)90149-8.

Grossman, J.N., Wasson, J.T., 1985. The origin and history of the metal and sulfide components of chondrules. *Geochimica et Cosmochimica Acta* 49, 925–939. doi:10.1016/0016-7037(85)90308-4.

Hasenstab, E., Tusch, J., Schnabel, C., Marien, C.S., Van Kranendonk, M.J., Smithies, H., Howard, H., Maier, W.D., Münker, C., 2020. Evolution of the early to late Archean mantle from Hf-Nd-Ce isotope systematics in basalts and komatiites from the Pilbara Craton. *Earth and Planetary Science Letters* 553, 116627. doi:10.1016/j.epsl.2020.116627.

Heck, P.R., Schmitz, B., Bottke, W.F., Rout, S.S., Kita, N.T., Cronholm, A., Defouilloy, C., Dronov, A., Terfelt, F., 2017. Rare meteorites common in the Ordovician period. *Nature Astronomy* 1, 0035. doi:10.1038/s41550-016-0035.

Hewins, R.H., Herzberg, C.T., 1996. Nebular turbulence, chondrule formation, and the composition of the Earth. *Earth and Planetary Science Letters* 144, 1–7. doi:10.1016/0012-821X(96)00159-8.

Hezel, D.C., Bland, P., Palme, H., Jacquet, E., Bigolski, J., 2018a. Composition of chondrules and matrix and their complementary relationship in chondrites, in: Russell, S.S., Connolly, Jr., H.C., Krot, A.N. (Eds.), *Chondrules and the Protoplanetary Disk*. Cambridge University Press, Cambridge. chapter 4, pp. 91–121. doi:10.1017/9781108284073.004.

Hezel, D.C., Harak, M., Libourel, G., 2018b. What we know about elemental bulk chondrule and matrix compositions: Presenting the ChondriteDB Database. *Chemie der Erde-Geochemistry* 78, 1–14. doi:10.1016/j.chemer.2017.05.003.

- Hezel, D.C., Parteli, E.J., 2018. The spatial origin of chondrules in individual chondrites: Constraints from modeling chondrule mixing. *The Astrophysical Journal* 863, 54. doi:10.3847/1538-4357/aad041.
- Horstmann, M., Humayun, M., Bischoff, A., 2014. Clues to the origin of metal in Almahata Sitta EL and EH chondrites and implications for primitive E chondrite thermal histories. *Geochimica et Cosmochimica Acta* 140, 720–744. doi:10.1016/j.gca.2014.04.041.
- Hsu, W., 1998. Geochemical and petrographic studies of oldhamite, diopside, and roedderite in enstatite meteorites. *Meteoritics & Planetary Science* 33, 291–301. doi:10.1111/j.1945-5100.1998.tb01633.x.
- Hutson, M., Ruzicka, A., 2000. A multi-step model for the origin of E3 (enstatite) chondrites. *Meteoritics & Planetary Science* 35, 601–608. doi:10.1111/j.1945-5100.2000.tb01440.x.
- Ikeda, Y., 1983. Major element chemical compositions and chemical types of chondrules in unequilibrated E, O, and C chondrites from Antarctica. *Memoirs of National Institute of Polar Research. Special issue* 30, 122–145.
- Ishida, H., Nakamura, T., Miura, H., Kakazu, Y., 2012. Diverse mineralogical and oxygen isotopic signatures recorded in CV3 carbonaceous chondrites. *Polar Science* 6, 252–262. doi:10.1016/j.polar.2012.06.002.
- Jacquet, E., Alard, O., Gounelle, M., 2015. The formation conditions of enstatite chondrites: Insights from trace element geochemistry of olivine-bearing chondrules in Sahara 97096 (EH3). *Meteoritics & Planetary Science* 50, 1624–1642. doi:10.1111/maps.12481.
- Jacquet, E., Piani, L., Weisberg, M.K., 2018. Chondrules in enstatite chondrites, in: Russell, S.S., Connolly, Jr., H.C., Krot, A.N. (Eds.), *Chondrules: Records of Protoplanetary Disk Processes*.

Cambridge University Press, Cambridge. volume 22. chapter 7, pp. 175–195. doi:10.1017/9781108284073.007.

Javoy, M., Kaminski, E., Guyot, F., Andrault, D., Sanloup, C., Moreira, M., Labrosse, S., Jambon, A., Agrinier, P., Davaille, A., Jaupart, C., 2010. The chemical composition of the Earth: Enstatite chondrite models. *Earth and Planetary Science Letters* 293, 259–268. doi:10.1016/j.epsl.2010.02.033.

Jochum, K.P., Nohl, U., 2008. Reference materials in geochemistry and environmental research and the GeoReM database. *Chemical Geology* 253, 50–53. doi:10.1016/j.chemgeo.2008.04.002.

Jochum, K.P., Weis, U., Stoll, B., Kuzmin, D., Yang, Q., Raczek, I., Jacob, D.E., Stracke, A., Birbaum, K., Frick, D.A., Günther, D., Enzweiler, J., 2011. Determination of reference values for NIST SRM 610–617 glasses following ISO guidelines. *Geostandards and Geoanalytical Research* 35, 397–429. doi:10.1111/j.1751-908X.2011.00120.x.

Johansen, A., Mac Low, M.M., Lacerda, P., Bizzarro, M., 2015. Growth of asteroids, planetary embryos, and Kuiper belt objects by chondrule accretion. *Science Advances* 1, e1500109. doi:10.1126/sciadv.1500109.

Johnson, T., Lofgren, G.E., 1995. Relative abundances of chondrule textural types in E3 chondrites, in: *Lunar and Planetary Science Conference*, pp. 689–690.

Jones, R.H., 2012. Petrographic constraints on the diversity of chondrule reservoirs in the protoplanetary disk. *Meteoritics & Planetary Science* 47, 1176–1190. doi:10.1111/j.1945-5100.2011.01327.x.

Kamber, B.S., Collerson, K.D., 2000. Role of 'hidden' deeply subducted slabs in mantle depletion. *Chemical Geology* 166, 241–254. doi:10.1016/S0009-2541(99)00218-1.

- Keil, K., 1968. Mineralogical and chemical relationships among enstatite chondrites. *Journal of Geophysical Research* 73, 6945–6976. doi:10.1029/JB073i022p06945.
- Kerridge, J., 1979. Fractionation of refractory lithophile elements among chondritic meteorites, in: *Lunar and Planetary Science Conference Proceedings*, pp. 989–996.
- Kimura, M., 1988. Origin of opaque minerals in an unequilibrated enstatite chondrite, Yamato-691. *Antarctic Meteorite Research* 1, 51–64.
- Kiseeva, E.S., Wood, B.J., 2015. The effects of composition and temperature on chalcophile and lithophile element partitioning into magmatic sulphides. *Earth and Planetary Science Letters* 424, 280–294. doi:10.1016/j.epsl.2015.05.012.
- Kornacki, A.S., Fegley, Jr., B., 1986. The abundance and relative volatility of refractory trace elements in Allende Ca, Al-rich inclusions: Implications for chemical and physical processes in the solar nebula. *Earth and Planetary Science Letters* 79, 217–234. doi:10.1016/0012-821X(86)90180-9.
- Krot, A.N., Nagashima, K., Petaev, M.I., 2012. Isotopically uniform, ^{16}O -depleted calcium, aluminum-rich inclusions in CH and CB carbonaceous chondrites. *Geochimica et Cosmochimica Acta* 83, 159–178. doi:10.1016/j.gca.2011.11.045.
- Krot, A.N., Petaev, M.I., Russell, S.S., Itoh, S., Fagan, T.J., Yurimoto, H., Chizmadia, L., Weisberg, M.K., Komatsu, M., Ulyanov, A.A., 2004. Amoeboid olivine aggregates and related objects in carbonaceous chondrites: Records of nebular and asteroid processes. *Chemie der Erde Geochemistry* 64, 185–239. doi:10.1016/j.chemer.2004.05.001.
- Krot, A.N., Scott, E.R.D., Goodrich, C.A., Weisberg, M.K., 2014. Chondrites and their Components, in: Holland, H.D., Turekian, K.K. (Eds.), *Treatise on Geochemistry* (Second Edition). Elsevier, Oxford. volume 1, pp. 1–63. doi:10.1016/B978-0-08-095975-7.00102-9.

Kruss, M., Wurm, G., 2018. Seeding the Formation of Mercurys: An Iron-sensitive Bouncing Barrier in Disk Magnetic Fields. *The Astrophysical Journal* 869, 45. doi:10.3847/1538-4357/aaec78.

Kruss, M., Wurm, G., 2020. Composition and size dependent sorting in preplanetary growth: seeding the formation of Mercury-like planets. *The Planetary Science Journal* 1, 23. doi:10.3847/PSJ/ab93c4.

Kuebler, K.E., McSween, Jr., H.Y., Carlson, W.D., Hirsch, D., 1999. Sizes and masses of chondrules and metal–troilite grains in ordinary chondrites: Possible implications for nebular sorting. *Icarus* 141, 96–106. doi:10.1006/icar.1999.6161.

Larimer, J.W., 1968. An experimental investigation of oldhamite, CaS; and the petrologic significance of oldhamite in meteorites. *Geochimica et Cosmochimica Acta* 32, 965–982. doi:10.1016/0016-7037(68)90061-6.

Larimer, J.W., 1975. The effect of C/O ratio on the condensation of planetary material. *Geochimica et Cosmochimica Acta* 39, 389–392. doi:10.1016/0016-7037(75)90204-5.

Larimer, J.W., 1979. The condensation and fractionation of refractory lithophile elements. *Icarus* 40, 446–454. doi:10.1016/0019-1035(79)90038-1.

Larimer, J.W., Bartholomay, M., 1979. The role of carbon and oxygen in cosmic gases: Some applications to the chemistry and mineralogy of enstatite chondrites. *Geochimica et Cosmochimica Acta* 43, 1455–1466. doi:10.1016/0016-7037(79)90140-6.

Larimer, J.W., Ganapathy, R., 1987. The trace element chemistry of CaS in enstatite chondrites and some implications regarding its origin. *Earth and Planetary Science Letters* 84, 123–134. doi:10.1016/0012-821X(87)90080-X.

Larimer, J.W., Wasson, J.T., 1988. Refractory lithophile elements, in: Kerridge, J.F., Matthews, M.S. (Eds.), *Meteorites and the Early Solar System*. University of Arizona Press, Tucson, pp. 394–415.

Lehner, S.W., Buseck, P.R., McDonough, W.F., 2010. Origin of kamacite, schreibersite, and perryite in metal-sulfide nodules of the enstatite chondrite Sahara 97072 (EH3). *Meteoritics & Planetary Science* 45, 289–303. doi:10.1111/j.1945-5100.2010.01027.x.

Lehner, S.W., McDonough, W.F., Németh, P., 2014. EH3 matrix mineralogy with major and trace element composition compared to chondrules. *Meteoritics & Planetary Science* 49, 2219–2240. doi:10.1111/maps.12391.

Lehner, S.W., Petaev, M.I., Zolotov, M.Y., Buseck, P.R., 2013. Formation of niningerite by silicate sulfidation in EH3 enstatite chondrites. *Geochimica et Cosmochimica Acta* 101, 34–56. doi:10.1016/j.gca.2012.10.003.

Levison, H.F., Kretke, K.A., Walsh, K.J., Bottke, W.F., 2015. Growing the terrestrial planets from the gradual accumulation of submeter-sized objects. *Proceedings of the National Academy of Sciences* 112, 14180–14185. doi:10.1073/pnas.1513364112.

Lin, Y., El Goresy, A., 2002. A comparative study of opaque phases in Qingzhen (EH3) and MacAlpine Hills 88136 (EL3): Representatives of EH and EL parent bodies. *Meteoritics & Planetary Science* 37, 577–599. doi:10.1111/j.1945-5100.2002.tb00840.x.

Lodders, K., 2003. Solar system abundances and condensation temperatures of the elements. *The Astrophysical Journal* 591, 1220–1247. doi:10.1086/375492.

Lodders, K., 2020. Solar Elemental Abundances, in: Read, P. (Ed.), *Oxford Research Encyclopedia of Planetary Science*. Oxford University Press, Oxford, pp. 1–68. doi:10.1093/acrefore/9780190647926.013.145.

Lodders, K., Fegley, Jr., B., 1993. Lanthanide and actinide chemistry at high C/O ratios in the solar nebula. *Earth and Planetary Science Letters* 117, 125–145. doi:10.1016/0012-821X(93)90122-P.

MacPherson, G.J., 2014. Calcium-aluminum-rich inclusions in chondritic meteorites, in: Holland, H.D., Turekian, K.K. (Eds.), *Meteorites and Cosmochemical Processes*. Elsevier, Oxford. volume 1 of *Treatise on Geochemistry (Second Edition)*, pp. 139–179. doi:10.1016/B978-0-08-095975-7.00105-4.

Mann, U., Frost, D.J., Rubie, D.C., 2009. Evidence for high-pressure core-mantle differentiation from the metal-silicate partitioning of lithophile and weakly-siderophile elements. *Geochimica et Cosmochimica Acta* 73, 7360–7386. doi:10.1016/j.gca.2009.08.006.

Margot, J.L., Hauck, I., Steven, A., Mazarico, E., Padovan, S., Peale, S.J., 2018. Mercury's internal structure, in: Solomon, S.C., Nittler, L.R., Anderson, B.J. (Eds.), *Mercury: The View after MESSENGER*. Cambridge University Press, Cambridge, pp. 85–113. doi:10.1017/9781316650684.005.

Mason, B., Martin, P.M., 1977. Geochemical differences among components of the Allende meteorite. *Smithsonian Contributions to the Earth Sciences* 19, 84–95. doi:10.5479/si.00810274.22.1.

McCoy, T.J., Dickinson, T.L., Lofgren, G.E., 1999. Partial melting of the Indarch (EH4) meteorite: A textural, chemical, and phase relations view of melting and melt migration. *Meteoritics & Planetary Science* 34, 735–746. doi:10.1111/j.1945-5100.1999.tb01386.x.

McDonough, W.F., 1991. Partial melting of subducted oceanic crust and isolation of its residual eclogitic lithology. *Philosophical Transactions of the Royal Society of London A: Mathematical, Physical and Engineering Sciences* 335, 407–418. doi:10.1098/rsta.1991.0055.

- McDonough, W.F., 2014. Compositional model for the Earth's core, in: Holland, H.D., Turekian, K.K. (Eds.), *Treatise on Geochemistry* (Second Edition). Elsevier, Oxford. volume 3, pp. 559–577. doi:10.1016/B978-0-08-095975-7.00215-1.
- McDonough, W.F., Sun, S.s., 1995. The composition of the Earth. *Chemical Geology* 120, 223–253. doi:10.1016/0009-2541(94)00140-4.
- Misawa, K., Nakamura, N., 1988a. Demonstration of REE fractionation among individual chondrules from the Allende (CV3) chondrite. *Geochimica et Cosmochimica Acta* 52, 1699–1710. doi:10.1016/0016-7037(88)90238-4.
- Misawa, K., Nakamura, N., 1988b. Highly fractionated rare-earth elements in ferromagnesian chondrules from the Felix (CO3) meteorite. *Nature* 334, 47–50. doi:10.1038/334047a0.
- Morbidelli, A., Libourel, G., Palme, H., Jacobson, S.A., Rubie, D.C., 2020. Subsolar Al/Si and Mg/Si ratios of non-carbonaceous chondrites reveal planetesimal formation during early condensation in the protoplanetary disk. *Earth and Planetary Science Letters* 538, 116220. doi:10.1016/j.epsl.2020.116220.
- Münker, C., Fonseca, R.O.C., Schulz, T., 2017. Silicate Earth's missing niobium may have been sequestered into asteroidal cores. *Nature Geoscience* 10, 822–826. doi:10.1038/ngeo3048.
- Münker, C., Pfänder, J.A., Weyer, S., Büchl, A., Kleine, T., Mezger, K., 2003. Evolution of planetary cores and the Earth-Moon system from Nb/Ta systematics. *Science* 301, 84–87. doi:10.1126/science.1084662.
- Namur, O., Charlier, B., Holtz, F., Cartier, C., McCammon, C., 2016. Sulfur solubility in reduced mafic silicate melts: Implications for the speciation and distribution of sulfur on Mercury. *Earth and Planetary Science Letters* 448, 102–114. doi:10.1016/j.epsl.2016.05.024.

- Nebel, O., van Westrenen, W., Vroon, P.Z., Wille, M., Raith, M.M., 2010. Deep mantle storage of the Earth's missing niobium in late-stage residual melts from a magma ocean. *Geochimica et Cosmochimica Acta* 74, 4392–4404. doi:10.1016/j.gca.2010.04.061.
- Nesbitt, R.W., Sun, S.S., Purvis, A.C., 1979. Komatiites; geochemistry and genesis. *The Canadian Mineralogist* 17, 165–186.
- Nittler, L.R., Chabot, N.L., Grove, T.L., Peplowski, P.N., 2018. The Chemical Composition of Mercury, in: Solomon, S.C., Nittler, L.R., Anderson, B.J. (Eds.), *Mercury: The View after MESSENGER*. Cambridge University Press, Cambridge, pp. 30–51. doi:10.1017/9781316650684.003.
- Nittler, L.R., Frank, E.A., Weider, S.Z., Crapster-Pregont, E., Vorburger, A., Starr, R.D., Solomon, S.C., 2020. Global major-element maps of Mercury from four years of MESSENGER X-Ray Spectrometer observations. *Icarus* , 113716doi:10.1016/j.icarus.2020.113716.
- Nittler, L.R., Starr, R.D., Weider, S.Z., McCoy, T.J., Boynton, W.V., Ebel, D.S., Ernst, C.M., Evans, L.G., Goldsten, J.O., Hamara, D.K., Lawrence, D.J., McNutt, R.L., Schlemm, C.E., Solomon, S.C., Sprague, A.L., 2011. The major-element composition of Mercury's surface from MESSENGER X-ray spectrometry. *Science* 333, 1847–1850. doi:10.1126/science.1211567.
- Osborn, T.W., Smith, R.H., Schmitt, R.A., 1973. Elemental composition of individual chondrules from ordinary chondrites. *Geochimica et Cosmochimica Acta* 37, 1909–1942. doi:10.1016/0016-7037(73)90149-X.
- Pack, A., Russell, S.S., Shelley, J.M.G., Van Zuilen, M., 2007. Geo- and cosmochemistry of the twin elements yttrium and holmium. *Geochimica et Cosmochimica Acta* 71, 4592–4608. doi:10.1016/j.gca.2007.07.010.
- Pack, A., Shelley, J.M.G., Palme, H., 2004. Chondrules with peculiar REE patterns: Implications

for solar nebular condensation at high C/O. *Science* 303, 997–1000. doi:10.1126/science.1092906.

Palme, H., Larimer, J.W., Lipschutz, M.E., 1988. Moderately volatile elements, in: Kerridge, J.F., Matthews, M.S. (Eds.), *Meteorites and the Early Solar System*. The University of Arizona Press, Tucson, pp. 436–461.

Palme, H., O'Neill, H.S.C., 2014. Cosmochemical estimates of mantle composition, in: Holland, H.D., Turekian, K.K. (Eds.), *Treatise on Geochemistry (Second Edition)*. Elsevier, Oxford. volume 3, pp. 1–39. doi:10.1016/B978-0-08-095975-7.00201-1.

Palme, H., Spettel, B., Hezel, D., 2014. Siderophile elements in chondrules of CV chondrites. *Chemie der Erde-Geochemistry* 74, 507–516. doi:10.1016/j.chemer.2014.06.003.

Pasek, M.A., Milsom, J.A., Ciesla, F.J., Lauretta, D.S., Sharp, C.M., Lunine, J.I., 2005. Sulfur chemistry with time-varying oxygen abundance during Solar System formation. *Icarus* 175, 1–14. doi:10.1016/j.icarus.2004.10.012.

Patzer, A., Hezel, D.C., Bendel, V., Pack, A., 2018. Chondritic ingredients: II. Reconstructing early solar system history via refractory lithophile trace elements in individual objects of the Leoville CV3 chondrite. *Meteoritics & Planetary Science* 53, 1391–1412. doi:10.1111/maps.13084.

Patzer, A., Pack, A., Gerdes, A., 2010. Zirconium and hafnium in meteorites. *Meteoritics & Planetary Science* 45, 1136–1151. doi:10.1111/j.1945-5100.2010.01076.x.

Peplowski, P.N., Evans, L.G., Hauck, S.A., McCoy, T.J., Boynton, W.V., Gillis-Davis, J.J., Ebel, D.S., Goldsten, J.O., Hamara, D.K., Lawrence, D.J., McNutt, R.L., Nittler, L.R., Solomon, S.C., Rhodes, E.A., Sprague, A.L., Starr, R.D., Stockstill-Cahill, K.R., 2011. Radioactive elements on Mercury's surface from MESSENGER: Implications for the planet's formation and evolution. *Science* 333, 1850–1852. doi:10.1126/science.1211576.

- Piani, L., Marrocchi, Y., Libourel, G., Tissandier, L., 2016. Magmatic sulfides in the porphyritic chondrules of EH enstatite chondrites. *Geochimica et Cosmochimica Acta* 195, 84–99. doi:10.1016/j.gca.2016.09.010.
- Quirico, E., Bourot-Denise, M., Robin, C., Montagnac, G., Beck, P., 2011. A reappraisal of the metamorphic history of EH3 and EL3 enstatite chondrites. *Geochimica et Cosmochimica Acta* 75, 3088–3102. doi:10.1016/j.gca.2011.03.009.
- Rambaldi, E.R., Wasson, J.T., 1981. Metal and associated phases in Bishunpur, a highly unequilibrated ordinary chondrite. *Geochimica et Cosmochimica Acta* 45, 1001–1015. doi:10.1016/0016-7037(81)90127-7.
- Rambaldi, E.R., Wasson, J.T., 1984. Metal and associated phases in Krymka and Chainpur: Nebular formation processes. *Geochimica et Cosmochimica Acta* 48, 1885–1897. doi:10.1016/0016-7037(84)90372-7.
- Rubie, D.C., Frost, D.J., Mann, U., Asahara, Y., Nimmo, F., Tsuno, K., Kegler, P., Holzheid, A., Palme, H., 2011. Heterogeneous accretion, composition and core–mantle differentiation of the Earth. *Earth and Planetary Science Letters* 301, 31–42. doi:10.1016/j.epsl.2010.11.030.
- Rubie, D.C., Jacobson, S.A., Morbidelli, A., O'Brien, D.P., Young, E.D., de Vries, J., Nimmo, F., Palme, H., Frost, D.J., 2015. Accretion and differentiation of the terrestrial planets with implications for the compositions of early-formed Solar System bodies and accretion of water. *Icarus* 248, 89–108. doi:10.1016/j.icarus.2014.10.015.
- Rubin, A.E., Scott, E.R.D., Keil, K., 1997. Shock metamorphism of enstatite chondrites. *Geochimica et Cosmochimica Acta* 61, 847–858. doi:10.1016/S0016-7037(96)00364-X.
- Rudnick, R.L., Barth, M., Horn, I., McDonough, W.F., 2000. Rutile-bearing refractory eclogites:

Missing link between continents and depleted mantle. *Science* 287, 278–281. doi:10.1126/science.287.5451.278.

Ruzicka, A., Floss, C., Hutson, M., 2012. Amoeboid olivine aggregates (AOAs) in the Efremovka, Leoville and Vigarano (CV3) chondrites: A record of condensate evolution in the solar nebula. *Geochimica et Cosmochimica Acta* 79, 79–105. doi:10.1016/j.gca.2011.11.043.

Satterwhite, C., Righter, K., 2007. Petrographic Descriptions. *Antarctic Meteorite Newsletter* 30, 18–30.

Schmidt, M.W., Dardon, A., Chazot, G., Vannucci, R., 2004. The dependence of Nb and Ta rutile–melt partitioning on melt composition and Nb/Ta fractionation during subduction processes. *Earth and Planetary Science Letters* 226, 415–432. doi:10.1016/j.epsl.2004.08.010.

Schneider, D.M., Symes, S.J.K., Benoit, P.H., Sears, D.W.G., 2002. Properties of chondrules in EL3 chondrites, comparison with EH3 chondrites, and the implications for the formation of enstatite chondrites. *Meteoritics & Planetary Science* 37, 1401–1416. doi:10.1111/j.1945-5100.2002.tb01037.x.

Schönbächler, M., Carlson, R.W., Horan, M.F., Mock, T.D., Hauri, E.H., 2010. Heterogeneous accretion and the moderately volatile element budget of Earth. *Science* 328, 884–887. doi:10.1126/science.1186239.

Sharp, C.M., Wasserburg, G.J., 1995. Molecular equilibria and condensation temperatures in carbon-rich gases. *Geochimica et Cosmochimica Acta* 59, 1633–1652. doi:10.1016/0016-7037(95)00069-C.

Steenstra, E.S., van Westrenen, W., 2020. Geochemical constraints on core-mantle differentiation in Mercury and the aubrite parent body. *Icarus* 340, 113621. doi:10.1016/j.icarus.2020.113621.

- Stracke, A., Palme, H., Gellissen, M., Münker, C., Kleine, T., Birbaum, K., Günther, D., Bourdon, B., Zipfel, J., 2012. Refractory element fractionation in the Allende meteorite: Implications for solar nebula condensation and the chondritic composition of planetary bodies. *Geochimica et Cosmochimica Acta* 85, 114–141. doi:10.1016/j.gca.2012.02.006.
- Sun, S.s., McDonough, W.F., 1989. Chemical and isotopic systematics of oceanic basalts: Implications for mantle composition and processes. Geological Society, London, Special Publications 42, 313–345. doi:10.1144/GSL.SP.1989.042.01.19.
- Uesugi, M., Sekiya, M., Nakamura, T., 2008. Kinetic stability of a melted iron globule during chondrule formation. I. Non-rotating model. *Meteoritics & Planetary Science* 43, 717–730. doi:10.1111/j.1945-5100.2008.tb00680.x.
- Urey, H.C., Craig, H., 1953. The composition of the stone meteorites and the origin of the meteorites. *Geochimica et Cosmochimica Acta* 4, 36–82. doi:10.1016/0016-7037(53)90064-7.
- Varela, M.E., Sylvester, P., Brandstätter, F., Engler, A., 2015. Nonporphyritic chondrules and chondrule fragments in enstatite chondrites: Insights into their origin and secondary processing. *Meteoritics & Planetary Science* 50, 1338–1361. doi:10.1111/maps.12468.
- Wade, J., Wood, B.J., 2001. The Earth's 'missing' niobium may be in the core. *Nature* 409, 75–78. doi:10.1038/35051064.
- Walker, R.J., McDonough, W.F., Honesto, J., Chabot, N.L., McCoy, T.J., Ash, R.D., Bellucci, J.J., 2008. Modeling fractional crystallization of group IVB iron meteorites. *Geochimica et Cosmochimica Acta* 72, 2198–2216. doi:10.1016/j.gca.2008.01.021.
- Wänke, H., Dreibus, G., 1994. Chemistry and accretion history of Mars. *Philosophical Transactions of the Royal Society of London. Series A, Mathematical and Physical Sciences* 349, 285–293. doi:10.1098/rsta.1994.0132.

- Warren, P.H., 2011. Stable-isotopic anomalies and the accretionary assemblage of the Earth and Mars: A subordinate role for carbonaceous chondrites. *Earth and Planetary Science Letters* 311, 93–100. doi:10.1016/j.epsl.2011.08.047.
- Wasson, J.T., Kallemeyn, G.W., 1988. Compositions of chondrites. *Philosophical Transactions of the Royal Society of London A: Mathematical, Physical and Engineering Sciences* 325, 535–544. doi:10.1098/rsta.1988.0066.
- Weisberg, M.K., Kimura, M., 2012. The unequilibrated enstatite chondrites. *Chemie der Erde-Geochemistry* 72, 101–115. doi:10.1016/j.chemer.2012.04.003.
- Willig, M., Stracke, A., 2019. Earth's chondritic light rare earth element composition: Evidence from the Ce–Nd isotope systematics of chondrites and oceanic basalts. *Earth and Planetary Science Letters* 509, 55–65. doi:10.1016/j.epsl.2018.12.004.
- Wipperfurth, S.A., Guo, M., Šrámek, O., McDonough, W.F., 2018. Earth's chondritic Th/U: Negligible fractionation during accretion, core formation, and crust-mantle differentiation. *Earth and Planetary Science Letters* 498, 196–202. doi:10.1016/j.epsl.2018.06.029.
- Wood, B.J., Kiseeva, E.S., 2015. Trace element partitioning into sulfide: How lithophile elements become chalcophile and vice versa. *American Mineralogist* 100, 2371–2379. doi:10.2138/am-2015-5358CCBYNCND.
- Wood, J.A., Hashimoto, A., 1993. Mineral equilibrium in fractionated nebular systems. *Geochimica et Cosmochimica Acta* 57, 2377–2388. doi:10.1016/0016-7037(93)90575-H.
- Wurm, G., Trieloff, M., Rauer, H., 2013. Photophoretic separation of metals and silicates: The formation of Mercury-like planets and metal depletion in chondrites. *The Astrophysical Journal* 769, 78. doi:10.1088/0004-637X/769/1/78.

Yoshizaki, T., McDonough, W.F., 2020. The composition of Mars. *Geochimica et Cosmochimica Acta* 273, 137–162. doi:10.1016/j.gca.2020.01.011.

Yoshizaki, T., McDonough, W.F., 2021. Earth and Mars—distinct inner solar system products. *Geochemistry* doi:10.1016/j.chemer.2021.125746. In press.

Yoshizaki, T., Nakashima, D., Nakamura, T., Park, C., Sakamoto, N., Ishida, H., Itoh, S., 2019. Nebular history of an ultrarefractory phase bearing CAI from a reduced type CV chondrite. *Geochimica et Cosmochimica Acta* 252, 39–60. doi:10.1016/j.gca.2019.02.034.

Zanda, B., Bourot-Denise, M., Perron, C., Hewins, R.H., 1994. Origin and metamorphic redistribution of silicon, chromium, and phosphorus in the metal of chondrites. *Science* 265, 1846–1849. doi:10.1126/science.265.5180.1846.

Supplementary materials for

Variable refractory lithophile element compositions of planetary building blocks: insights from components of enstatite chondrites

Takashi Yoshizaki^{*1}, Richard D. Ash², Marc D. Lipella², Tetsuya Yokoyama³, and
William F. McDonough^{1,2,4}

¹Department of Earth Science, Graduate School of Science, Tohoku University, Sendai, Miyagi
980-8578, Japan

²Department of Geology, University of Maryland, College Park, MD 20742, USA

³Department of Earth and Planetary Sciences, Tokyo Institute of Technology, Ookayama, Tokyo
152-8851, Japan

⁴Research Center for Neutrino Science, Tohoku University, Sendai, Miyagi 980-8578, Japan

(*Corresponding author. E-mail: tky@dc.tohoku.ac.jp)

June 1, 2021

Appendix A Supplementary tables

Supplementary tables listed below are provided as Microsoft Excel spreadsheets.

Table A.1: Chemical composition of chondrules from primitive enstatite chondrites.

Table A.2: Chemical composition of troilite from primitive enstatite chondrites.

Table A.3: Chemical composition of oldhamite and niningerite from primitive enstatite chondrites.

Table A.4: Chemical composition of refractory inclusions from carbonaceous chondrites.

Table E.5: Summary of element ratios of chondrules from unequilibrated enstatite, ordinary, and carbonaceous chondrites.

Appendix B Supplementary text

B.1 Scanning electron microscope and electron microprobe analyses

Mineralogy and petrology of polished sections of the enstatite chondrite samples (Table 1) were analyzed using Hitachi S-3400N scanning electron microscope (SEM) and JEOL JSM-7001F field-emission (FE) SEM at Tohoku University (TU). Semi-quantitative analyses of constituent minerals and X-ray mapping were performed using Oxford INCA energy-dispersive spectrometers (EDS) equipped with the SEM instruments, at an accelerating voltage of 15 kV and a beam current of 1.0–1.4 nA.

Quantitative X-ray microanalysis of chondrules from enstatite chondrites and refractory inclusions from RBT 04143 was performed using JEOL JXA-8530F FE-type electron probe microanalyzer (EPMA) and JEOL JXA-8800 EPMA equipped with wavelength-dispersive X-ray spectrometers (WDS) at TU. A defocused electron beam (20–200 µm in diameter) with an acceleration voltage of 15 kV and beam current of 10 nA was used to determine abundances of 13 elements (Si, Ti, Al, Cr, Fe, Mn, Mg, Ca, Na, K, S, P and Ni) in bulk chondrules. The peak counting times were 10 s for Na; 20 s for Si, Al, Mg and Ca; and 40 s for Ti, Cr, Fe, Mn, K, P and Ni. To obtain bulk chemical composition, chondrules larger than 200 µm in diameter were measured multiple (up to 11) times and the average value was calculated. Well-characterized natural and synthetic crystalline oxides and metals were used as standards. Matrix corrections were applied using the atomic number (Z), absorption (A), and fluorescence (F) (ZAF) correction method. The detection limits of measurements using the JXA-8530F FE-EPMA were 0.02 wt% for CaO and K₂O; 0.03 wt% for SiO₂, MgO and Na₂O; 0.04 wt% for Al₂O₃, Cr₂O₃, FeO, MnO and P₂O₅; 0.05 wt% for NiO; 0.07 wt% for SO₃; and 0.16 wt% for TiO₂. The detection limits of analyses by the JXA-8800 EPMA were 0.01 wt% for CaO and K₂O; 0.02 wt% for Al₂O₃, Na₂O and SO₃; 0.03 wt% for MnO and MgO; 0.04 wt% for SiO₂, TiO₂, Cr₂O₃ and FeO; and 0.05 wt% for P₂O₅ and NiO.

A focused electron beam ($\sim 3 \mu\text{m}$ in diameter) accelerated at 15 kV with a beam current of 10 nA was used to quantify 13 elements (Si, Ti, Al, Cr, Fe, Mn, Mg, Ca, Na, K, P, Ni and S) in sulfides using the JXA-8800 EPMA at TU. Peak counting time was 20 s for all elements. Other analytical conditions were similar to those of chondrule measurements. Detection limits were 0.01 wt% for Si, Al, Mg, Ca, K, P and S; 0.02 wt% for Ti and Na; 0.03 wt% for Cr, Fe and Mn; and 0.04 wt% for Ni.

Major element abundance in refractory inclusions from Allende was determined using and JEOL JXA-8900R EPMA at University of Maryland. Analyses were performed in a semi-quantitative mode. Wavelength scans were performing with the following conditions: 15 kV accelerating potential, 150 nA cup current, and a 20 μm beam diameter. Raw X-ray intensities were corrected using the ZAF algorithm.

B.2 Comparison of the bulk chemical composition of EC chondrules with previous data

We recognize that the bulk composition of individual chondrules derived by surface analytical methods (i.e., broadened or scanning beam measurements on thin or thick sections) can be less accurate than those determined by a whole-rock measurement of mechanically separated chondrules. In particular, a biased sampling of phases in chondrules can provide RLE data that are affected by melt-crystal elemental fractionations. Thus, the ratios of elements with different incompatibilities (e.g., Al/Ti, Ca/Al, Nb/La, Sm/Nd) can be sensitive to the biased surface sampling, whereas those of the geochemical twins (Nb/Ta, Zr/Hf, and Y/Ho) might remain to represent the bulk chondrule compositions.

Recently, Gerber (2012) obtained bulk compositions of eight chondrules from type 4 EH Indarch, by analyzing solutions of mechanically isolated individual chondrules using ICP-MS and

ICP-OES. Although the number of data reported by Gerber (2012) is limited and all of them are obtained from a metamorphosed type 4 EH, they can be used to investigate representativeness of the bulk chondrule data obtained by the surface analytical methods. Our data of Nb/La, Zr/Hf, Al/Ti, and Ca/Al in EC chondrules are consistent with those from Gerber (2012) (Fig. B.1). EH4 chondrules from Gerber (2012) show slightly higher Y/Ho and Sm/Nd ratios than our data for EH3 and EL3 chondrules, which might reflect modifications of these ratios due to distinct behavior of these elemental twins during thermal processing in the EC parent bodies (Barrat et al., 2014).

Varela et al. (2015) obtained bulk chemical compositions of non-porphyritic chondrules from EH3 (Sahara 97158) and EH4 (Indarch) using the electron microprobe and LA-ICP-MS techniques. In general, their data are also consistent with data obtained by this study and Gerber (2012) (Fig. B.1). On the other hand, Varela et al. (2015) reported elevated Zr/Hf and low Al/Ti ratios of EH3 chondrule as compared to our results, whereas in EH4 these ratios are consistent with the results of Gerber (2012). Ratios of major RLE in type 3 EC obtained in this study are also consistent with electron microprobe data from Grossman et al. (1985) (Qingzhen (EH3)) and Schneider et al. (2002) (Allan Hills (ALH) 85119 (EL3); MacAlpine Hills (MAC) 88180 (EL3), and Pecora Escarpment (PCA) 91020 (EL3), PCA 91238)).

In contrast, electron microprobe data of bulk chondrules from Yamato 691 (EH3) obtained by Ikeda (1983) show wide spread in Al/Ti and Ca/Al ratios, with mean values overlapping the CI ratios (Fig. B.1). Since the data reported by Ikeda (1983) show lower Na and Al abundances compared to other studies (this study; Grossman et al., 1985; Gerber, 2012; Varela et al., 2015; Fig. B.2), it is likely that their data are derived from glass-poor regions of the EC chondrules. Ikeda (1983) noted that they avoided a beam overlap onto metals and sulfides in chondrules, which might also have led exclusion of a glassy mesostasis in which these opaque phases commonly enclosed (Weisberg and Kimura, 2012; Lehner et al., 2013; Piani et al., 2016; Jacquet et al., 2018). We also avoided a beam overlap onto these opaque phases in our measurements, in which high spatial resolution images from

optical and electron microscopes helped us to measure compositions of glassy areas without hitting sulfides. Alternatively, these discrepancies might represent unique compositional characteristics of chondrules from Yamato 691. Otherwise, our measurements might have overestimated the Al abundance, whereas our bulk Al/Ti and Ca/Al data are consistent with those from Gerber (2012). Thus, we consider that the consistency of our bulk chondrule data with those of Gerber (2012) support representative sampling of bulk chondrule minerals in our measurements.

B.3 Composition of troilites from ALHA77295

Troilites from ALH 84170 and ALH 84206 (EH3) have relatively uniform compositions, particularly for V through Mo (Fig. 5). Likewise, most of the troilites from ALHA77295 (EH3), show comparable abundance patterns, but are depleted in Nb ($0.1\text{--}0.8 \times \text{CI}$) as compared to other EH3 samples. However, in three of the analyzed troilites from ALHA77295 (i.e., $\sim 5\%$ of the total troilite signal for ALHA77295) we encountered marked increases in Nb + Ta \pm Mo \pm W signals during the laser ablation analyses. These compositionally heterogeneous domains are of the order of 5 cubic microns and typically these inclusions had marked enrichment in $\sim 500 \mu\text{g/g}$ Nb, nearly chondritic Nb/Ta, and order ppm levels of Mo and W. Such inclusions were not encountered during analysis of troilite from any of the other EH3 and EL3 chondrites. No significant signal change was detected for the major elements when we encounter the heterogeneous domains.

We found that the Nb concentration of bulk rock and of the acid leachate of ALHA77295 were similar to those of other unequilibrated EH chondrites (this study; Barrat et al., 2014). In ALHA77295 it is likely that some small fraction of the Nb and Ta and to a lesser extent Mo and W are hosted in these micron scale inclusions in troilite. We examined the post-ablation sampling area using FE-SEM/EDS, and found no additional metallic/sulfide inclusions. Therefore, the abundances of these elements in troilite from ALHA77295 reported in Fig. 5 should be considered as lower limits of their true concentrations.

B.4 Mineralogy and trace element chemistry of refractory inclusions from CV chondrites

Here we provide a brief description of mineralogy and chemistry of refractory inclusions (three CAI and six AOA) from CV chondrites analyzed in this study (Fig. B.5 and Table A.4). AOA are one of the most common type of refractory inclusions in carbonaceous chondrites (e.g., Krot et al., 2014). They are aggregates of fine-grained forsterite, Fe, Ni-metal and a variety of refractory minerals (e.g., Al-rich diopside, anorthite, spinel) (e.g., Krot et al., 2004). Geochemical investigation of AOA indicate that these inclusions are nebular condensates that have no or minor degree of melting after their formation (e.g., Krot et al., 2004), and thus they are considered to record fractionation of refractory elements occurred in the solar nebula (e.g., Ruzicka et al., 2012).

R7C-01 is a fragment of an irregularly shaped CAI that consists of fine-grained spinel and Al, Ti-rich diopside and a small amount of anorthite and surrounded by an Al-rich diopside rim. Anorthite is partially replaced by a secondary nepheline. The bulk CAI shows almost flat REE pattern ($\sim 40 \times \text{CI}$) with negative anomalies in Eu and Yb and a small negative Ce anomaly.

Based on mineralogy and bulk major element abundance, we classified AOA from RBT 04143 into two groups: Ca, Al-rich AOA and olivine-rich AOA. Ca, Al-rich AOA contain abundant nodules of Ca, Al-rich minerals that commonly occur in CAI (e.g., Al-diopside, anorthite, spinel; Brearley and Jones, 1998; MacPherson, 2014) with high bulk abundance of major RLE (e.g., Ca, Al, Ti; Table A.4). In contrast, such refractory minerals are nearly absent in olivine-rich AOA, which consist of abundant olivine and minor amounts of Fe, Ni-metal and Al-diopside.

R1A-03 is an irregularly-shaped Ca, Al-rich AOA that is composed of anorthite-rich nodules with minor Al, Ti-rich diopside and spinel, and forsterite. This inclusion has a nearly flat REE pattern ($\sim 5 \times \text{CI}$) with positive Ce and Eu anomalies. R4A-45 consists of a subrounded nodule that consists of a core of spinel + Al, Ti-rich diopside and Al-diopside rim, which is surrounded

by a compact-textured forsterite thereafter. Spinel-rich domain of this inclusion is characterized by highly fractionated REE pattern with a higher light REE abundance (Ce, Pr and Nd; $\sim 20 \times$ CI) than heavy REE (Gd, Tb, Dy, Ho, Er and Lu; $\sim 10 \times$ CI), and negative Eu and positive Sm, Tm and Yb anomalies. Two spot data were obtained from olivine-rich region of this inclusion. One measurement shows highly fractionated REE pattern as observed in the spinel-rich domain of this inclusion with much lower REE abundance ($\sim 5 \times$ CI and $\sim 2 \times$ CI for LREE and HREE, respectively). Another area of the olivine-rich domain shows nearly flat REE pattern ($\sim 5 \times$ CI) with a negative Eu anomaly.

Four AOA from RBT 04143 are classified as olivine-rich AOA. Typical CAI minerals (e.g., Al, Ti-rich diopside, spinel) are nearly absent in these inclusions. R3A-18 is irregularly-shaped, olivine-rich inclusion with a compact texture with low REE abundance. R1A-04 is a fine-grained irregular AOA which consists of forsterite-rich core and a mantle of forsterite + Fe-rich olivine + Fe, Ni-metal. The core of this inclusion is characterized by nearly flat REE pattern ($\sim 2 \times$ CI). R1A-01 is irregularly shaped AOA that is dominated by forsterite with a minor amount of Fe, Ni-metal. The REE pattern of this inclusion is flat ($\sim 4 \times$ CI) with negative Eu anomaly. R1A-06 is irregularly-shaped AOA that consists of Fe, Ni-metal-rich core, forsterite-rich mantle with minor Al-diopside, and a rim of forsterite + Fe, Ni-metal. This inclusion shows flat REE pattern ($\sim 1\text{--}2 \times$ CI).

For Allende CAI, we determined abundances of major elements and HFSE (Table A.4). The Allende CAI 3529-63-RR1 is a brecciated CAI with abundant spinel and anorthite. In this inclusion, anorthite occurs replacing primary melilite and minor Al, Ti-rich diopside is also identified. 3529-61-RR1 is a melilite-rich CAI with a well-developed rim sequence. Ca, Fe-rich pyroxene and sodalite is abundant in this inclusion, reflecting significant alteration of this inclusion in the Allende parent body.

Table B.1: Long-term precision of LA-ICP-MS analyses. Abbreviations: CC—carbonaceous chondrites; EC—enstatite chondrites.

Element	Mass	RSD%	Element	Mass	RSD%	Element	Mass	RSD%
NIST 610 (for EC chondrules and CC refractory inclusions, $n = 28$)								
Ca	43	4	Ce	140	3	Ho	165	5
Sc	45	4	Pr	141	3	Er	166	4
Ti	47	5	Nd	146	3	Tm	169	5
V	51	5	Sm	147	4	Yb	172	4
Y	89	4	Eu	151	4	Lu	175	3
Zr	90	4	Gd	157	4	Hf	178	2
Nb	93	4	Tb	159	6	Ta	181	3
Ba	137	5	Dy	163	5	W	182	4
La	139	3						
NIST 610 (for EC sulfides, $n = 32$)								
Mg	25	3	Ga	69	2	Sm	147	3
Al	27	4	Sr	88	3	Eu	153	4
Si	29	3	Y	89	4	Gd	157	4
P	31	3	Zr	90	3	Ho	165	4
Ca	43	3	Nb	93	3	Tm	169	4
Sc	45	3	Mo	95	4	Yb	172	4
Ti	47	4	Cs	133	4	Lu	175	3
V	51	3	La	139	4	Hf	178	3
Cr	53	3	Ce	140	4	Ta	181	3
Mn	55	3	Nd	146	4	W	182	4
Zn	66	2						
Filomena (for EC sulfides, $n = 32$)								
Ni	60	10						
Cu	63	8						

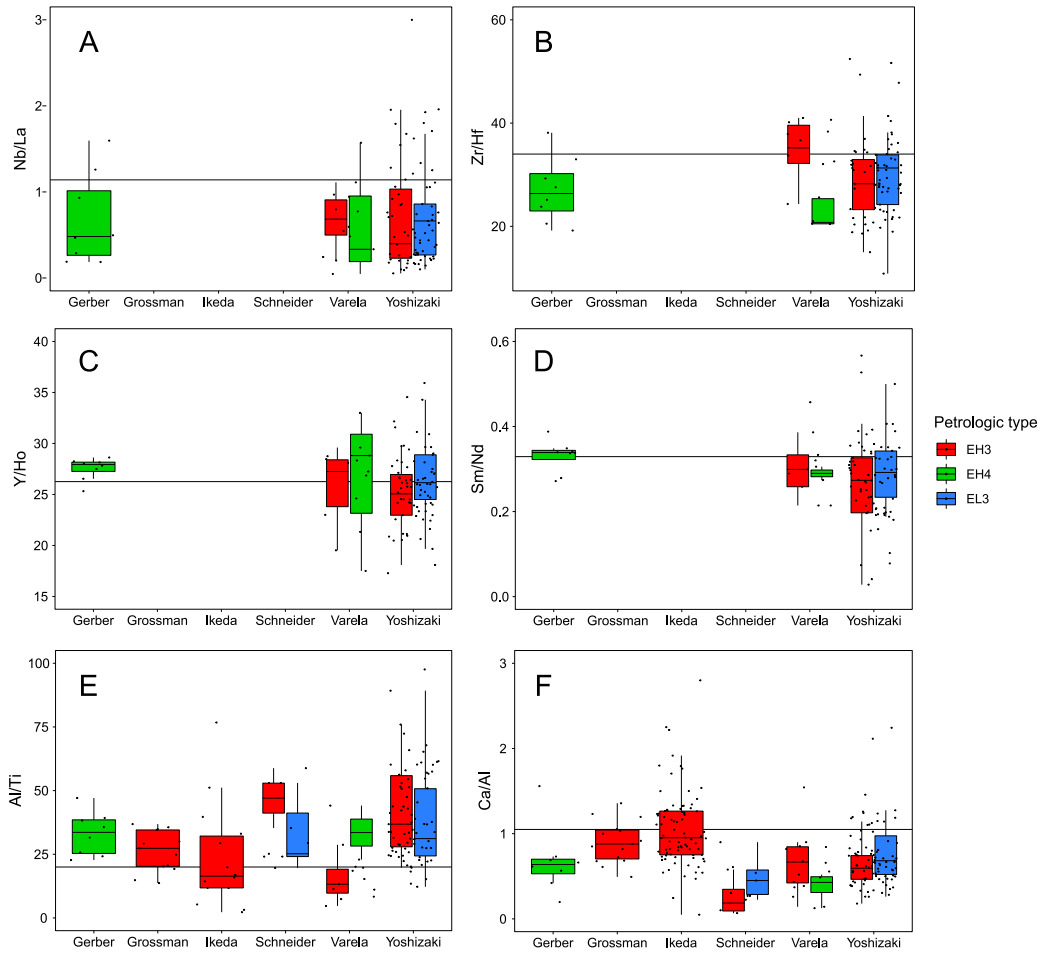


Fig. B.1: Ratios of refractory lithophile elements in the bulk chondrules from EH3 (red), EH4 (green), and EL3 (blue) chondrites (this study; Ikeda, 1983; Grossman et al., 1985; Schneider et al., 2002; Gerber, 2012; Varela et al., 2015). Horizontal lines represent the CI ratio (Lodders, 2020).

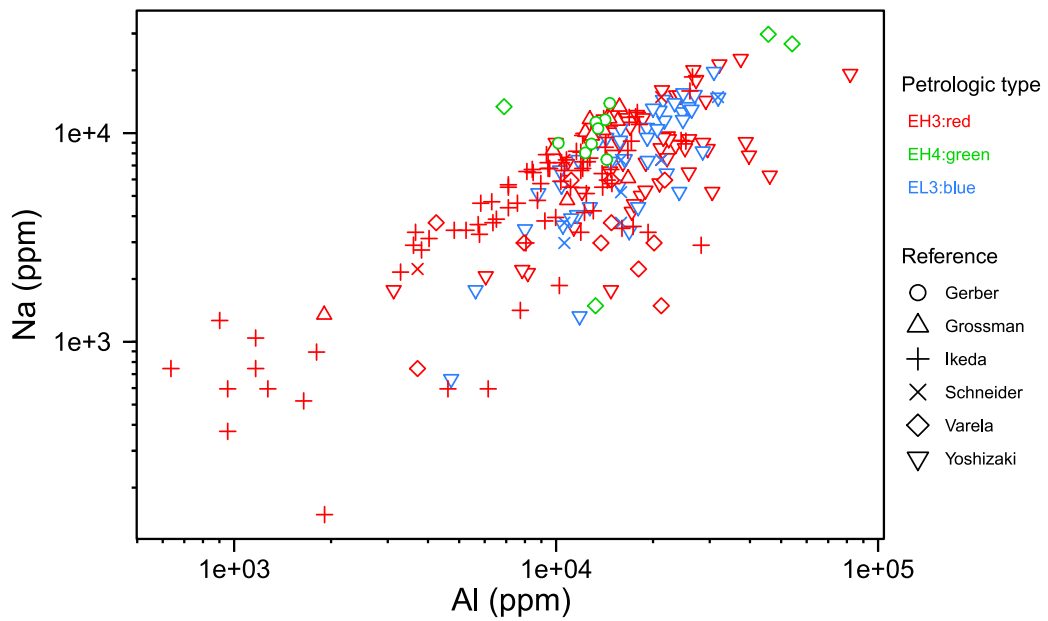


Fig. B.2: Abundances of Na and Al in bulk chondrules from EH3 (red), EH4 (green), and EL3 (blue) chondrites (this study; Ikeda, 1983; Grossman et al., 1985; Schneider et al., 2002; Gerber, 2012; Varela et al., 2015).

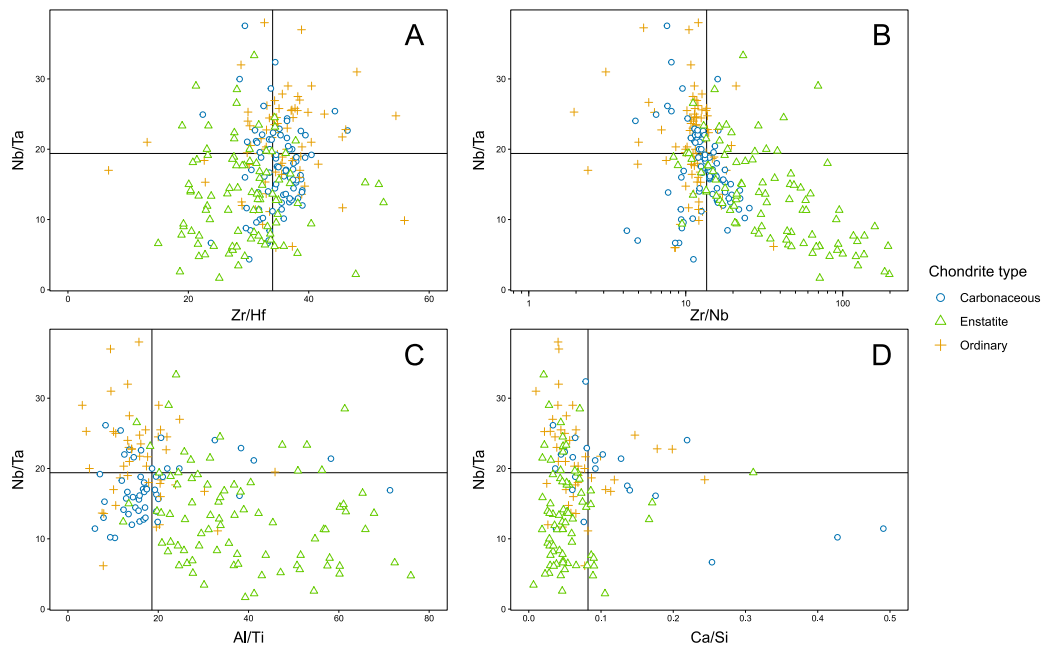


Fig. B.3: Lithophile element ratios vs Nb/Ta in chondrules from enstatite (green), ordinary (orange), and carbonaceous (blue) chondrites. Data sources are similar to those of Fig. 4.

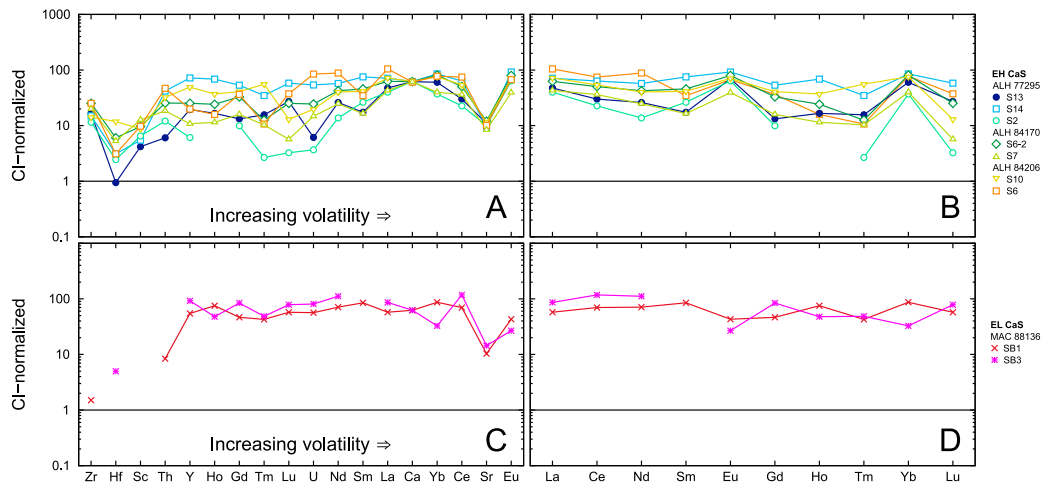


Fig. B.4: CI-normalized (Lodders, 2020) abundances of lithophile elements in oldhamites (CaS) from EH (A,B) and EL (C,D) chondrites. In (A) and (B), elements are arranged in the order of increasing volatility (Lodders, 2003).

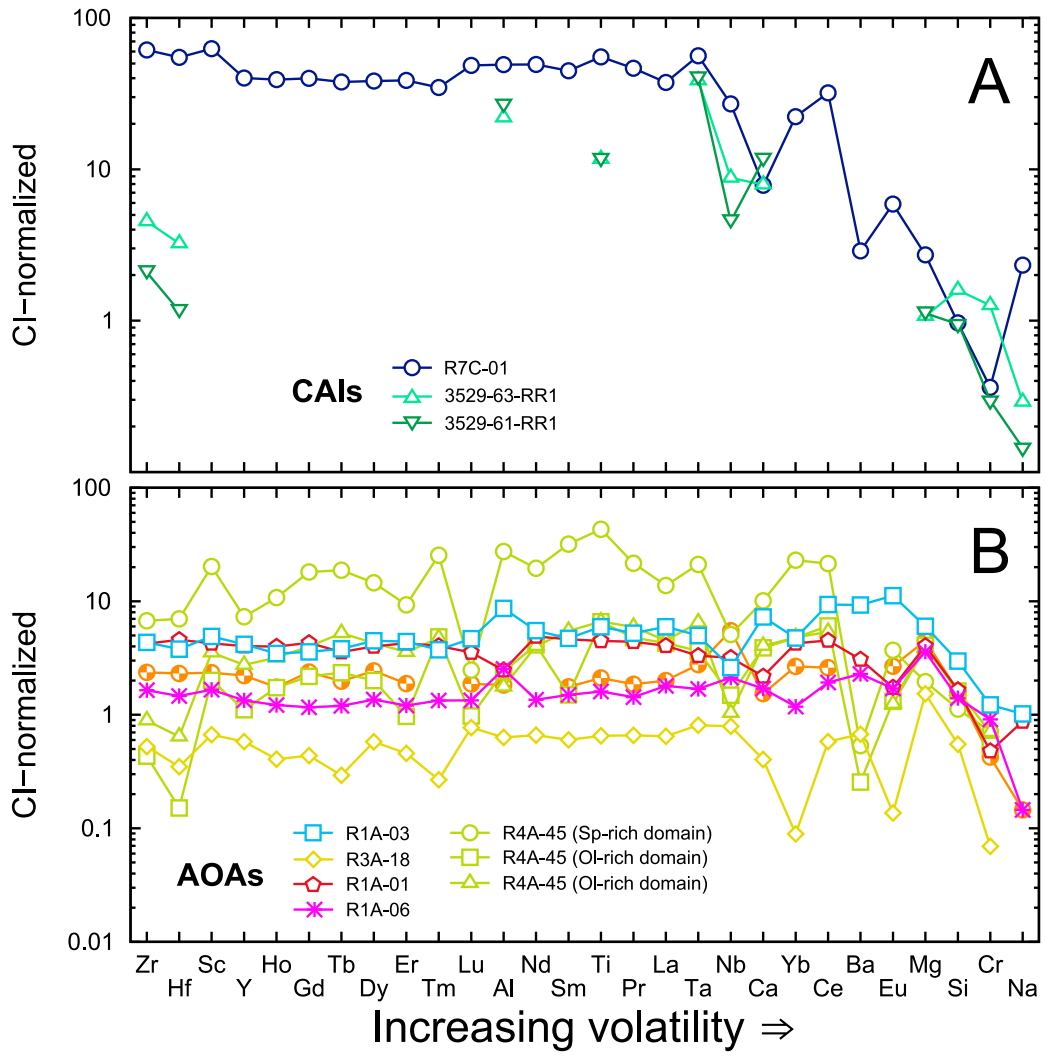


Fig. B.5: CI-normalized (Lodders, 2020) abundances of lithophile elements in (A) Ca, Al-rich inclusions (CAI) and (B) amoeboid olivine aggregates (AOA) from unequilibrated carbonaceous chondrites. Abbreviations: Ol—olivine; Sp—spinel.

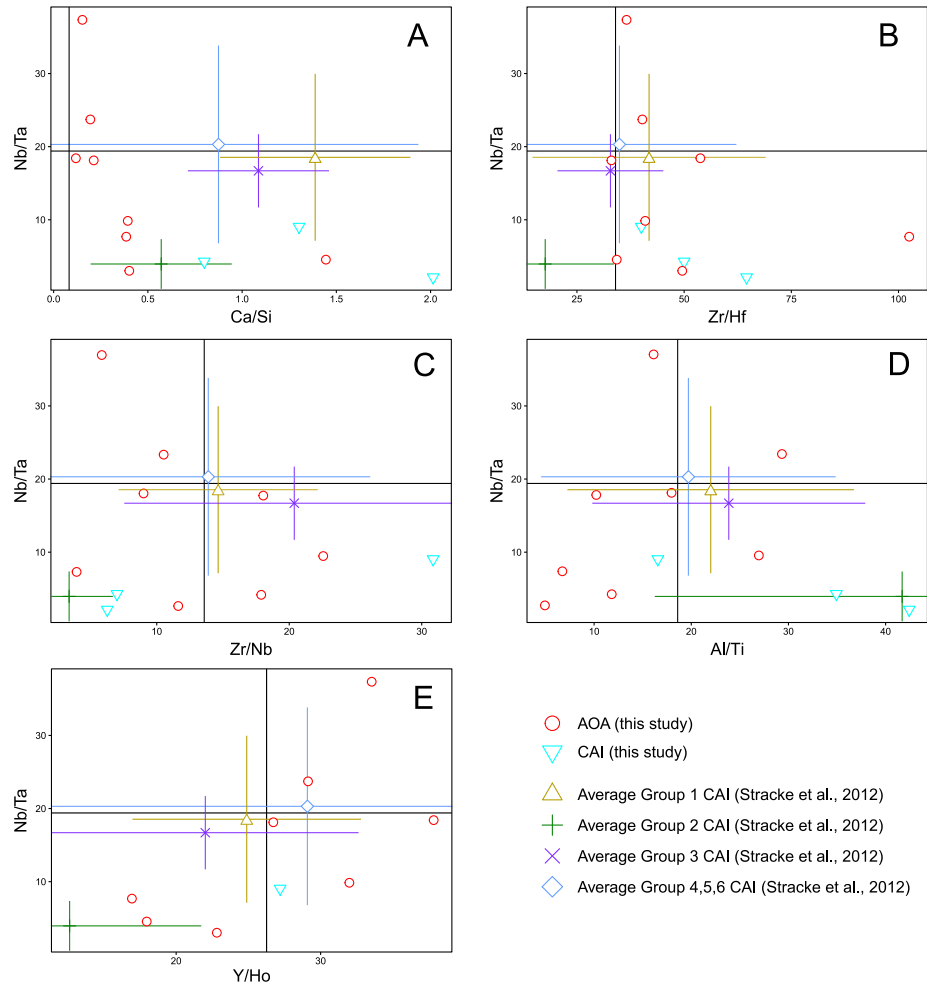


Fig. B.6: Lithophile element ratios of bulk refractory inclusions (CAI and AOA) from CV chondrites obtained in this study. Also shown are average compositions with 1 standard deviations of each group of CAI (Stracke et al., 2012).

Appendix C Sources of chondrule data

Here we provide a list of sources of literature chondrule data used to produce Fig. 4. Most of these literature data are obtained through the online database MetBase (<https://metbase.org/>).

- Becker, M., Hezel, D.C., Schulz, T., Elfers, B.M., Münker, C., 2015. Formation timescales of CV chondrites from component specific Hf–W systematics. *Earth and Planetary Science Letters* 432, 472–482. doi:10.1016/j.epsl.2015.09.049.
- Berlin, J., 2010. Mineralogy and bulk chemistry of chondrules and matrix in petrologic type 3 chondrites: Implications for early solar system processes. Ph.D. thesis. University of New Mexico.
- Beyersdorf-Kuis, U., 2014. Pre-irradiation of chondrules in the early solar system. Ph.D. thesis. Ruprecht-Karls-Universität, Heidelberg.
- Bischoff, A., Palme, H., Schultz, L., Weber, D., Weber, H.W., Spettel, B., 1993. Acfer 182 and paired samples, an iron-rich carbonaceous chondrite: Similarities with ALH85085 and relationship to CR chondrites. *Geochimica et Cosmochimica Acta* 57, 2631–2648. doi:10.1016/0016-7037(93)90422-S.
- Bridges, J.C., Franchi, I.A., Hutchison, R., Morse, A.D., Long, J.V.P., Pillinger, C.T., 1995. Cristobalite-and tridymite-bearing clasts in Parnallee (LL3) and Farmington (L5). *Meteoritics* 30, 715–727. doi:10.1111/j.1945-5100.1995.tb01169.x.
- Dodd, R.T., 1978. The composition and origin of large microporphyritic chondrules in the Manych (L-3) chondrite. *Earth and Planetary Science Letters* 39, 52–66. doi:10.1016/0012-821X(78)90140-1.

- Ebel, D.S., Weisberg, M.K., Hertz, J., Campbell, A.J., 2008. Shape, metal abundance, chemistry, and origin of chondrules in the Renazzo (CR) chondrite. *Meteoritics & Planetary Science* 43, 1725–1740. doi:10.1111/j.1945-5100.2008.tb00639.x.
- Ebert, S., Bischoff, A., 2016. Genetic relationship between Na-rich chondrules and Ca, Al-rich inclusions?—Formation of Na-rich chondrules by melting of refractory and volatile precursors in the solar nebula. *Geochimica et Cosmochimica Acta* 177, 182–204. doi:10.1016/j.gca.2016.01.014.
- Engler, A., Varela, M.E., Kurat, G., Ebel, D., Sylvester, P., 2007. The origin of non-porphyritic pyroxene chondrules in UOCs: Liquid solar nebula condensates? *Icarus* 192, 248–286. doi:10.1016/j.icarus.2007.06.016.
- Fredriksson, K., Brenner, P.R., Fredriksson, B.J., Olsen, E., 1997. A nondestructive analytical method for stone meteorites—And a controversial discrepancy. *Meteoritics & Planetary Science* 32, 55–60. doi:10.1111/j.1945-5100.1997.tb01240.x.
- Fujimaki, H., Matsu-Ura, M., Sunagawa, I., Aoki, K.i., 1981. Chemical compositions of chondrules and matrices in the ALH-77015 chondrite (L3). *Memoirs of National Institute of Polar Research. Special issue* 20, 161–174.
- Gerber, M., 2012. Chondrule formation in the early Solar System: A combined ICP-MS, ICP-OES and petrological study. Ph.D. thesis. University of Münster.
- Gooding, J.L., Keil, K., Fukuoka, T., Schmitt, R.A., 1980. Elemental abundances in chondrules from unequilibrated chondrites: Evidence for chondrule origin by melting of pre-existing materials. *Earth and Planetary Science Letters* 50, 171–180. doi:10.1016/0012-821X(80)90127-2.
- Grossman, J.N., Alexander, C.M.O., Ash, R.D., McDonough, W.F., 2007. Volatile element abun-

dances in chondrules revisited: An LA-ICP-MS study of QUE 97008 (LL3.05), in: Lunar and Planetary Science Conference, p. 2000.

Grossman, J.N., Rubin, A.E., Rambaldi, E.R., Rajan, R.S., Wasson, J.T., 1985. Chondrules in the Qingzhen type-3 enstatite chondrite: Possible precursor components and comparison to ordinary chondrite chondrules. *Geochimica et Cosmochimica Acta* 49, 1781–1795. doi:10.1016/0016-7037(85)90149-8.

Grossman, J.N., Wasson, J.T., 1983. Refractory precursor components of Semarkona chondrules and the fractionation of refractory elements among chondrites. *Geochimica et Cosmochimica Acta* 47, 759–771. doi:10.1016/0016-7037(83)90109-6.

Grossman, J.N., Wasson, J.T., 1987. Compositional evidence regarding the origins of rims on Semarkona chondrules. *Geochimica et Cosmochimica Acta* 51, 3003–3011. doi:10.1016/0016-7037(87)90373-5.

Hezel, D.C., Kießwetter, R., 2010. Quantifying the error of 2D bulk chondrule analyses using a computer model to simulate chondrules (SIMCHON). *Meteoritics & Planetary Science* 45, 555–571. doi:10.1111/j.1945-5100.2010.01040.x.

Hezel, D.C., Palme, H., 2008. Constraints for chondrule formation from Ca–Al distribution in carbonaceous chondrites. *Earth and Planetary Science Letters* 265, 716–725. doi:10.1016/j.epsl.2007.11.003.

Hezel, D.C., Palme, H., 2010. The chemical relationship between chondrules and matrix and the chondrule matrix complementarity. *Earth and Planetary Science Letters* 294, 85–93. doi:10.1016/j.epsl.2010.03.008.

Hezel, D.C., Palme, H., Nasdala, L., Brenker, F.E., 2006. Origin of SiO₂-rich components in or-

dinary chondrites. *Geochimica et Cosmochimica Acta* 70, 1548–1564. doi:10.1016/j.gca.2005.11.026.

Holland, G., Bridges, J.C., Busfield, A., Jeffries, T., Turner, G., Gilmour, J.D., 2005. Iodine-xenon analysis of Chainpur (LL3.4) chondrules. *Geochimica et Cosmochimica Acta* 69, 189–200. doi:10.1016/j.gca.2004.06.021.

Huang, S., Lu, J., Prinz, M., Weisberg, M.K., Benoit, P.H., Sears, D.W.G., 1996. Chondrules: Their diversity and the role of open-system processes during their formation. *Icarus* 122, 316–346. doi:10.1006/icar.1996.0127.

Ikeda, Y., 1983. Major element chemical compositions and chemical types of chondrules in unequilibrated E, O, and C chondrites from Antarctica. *Memoirs of National Institute of Polar Research. Special issue* 30, 122–145.

Ivanova, M.A., Kononkova, N.N., Krot, A.N., Greenwood, R.C., Franchi, I.A., Verchovsky, A.B., Trieloff, M., Korochantseva, E.V., Brandstätter, F., 2008. The Isheyev meteorite: Mineralogy, petrology, bulk chemistry, oxygen, nitrogen, carbon isotopic compositions, and ^{40}Ar - ^{39}Ar ages. *Meteoritics & Planetary Science* 43, 915–940. doi:10.1111/j.1945-5100.2008.tb01090.x.

Jones, R.H., 1990. Petrology and mineralogy of type II, FeO-rich chondrules in Semarkona (LL3.0): Origin by closed-system fractional crystallization, with evidence for supercooling. *Geochimica et Cosmochimica Acta* 54, 1785–1802. doi:10.1016/0016-7037(90)90408-D.

Jones, R.H., 1994. Petrology of FeO-poor, porphyritic pyroxene chondrules in the Semarkona chondrite. *Geochimica et Cosmochimica Acta* 58, 5325–5340. doi:10.1016/0016-7037(94)90316-6.

Jones, R.H., 1996. FeO-rich, porphyritic pyroxene chondrules in unequilibrated ordinary chon-

drites. *Geochimica et Cosmochimica Acta* 60, 3115–3138. doi:10.1016/0016-7037(96)00152-4.

Jones, R.H., Schilk, A.J., 2009. Chemistry, petrology and bulk oxygen isotope compositions of chondrules from the Mokoia CV3 carbonaceous chondrite. *Geochimica et Cosmochimica Acta* 73, 5854–5883. doi:10.1016/j.gca.2009.06.029.

Kimura, M., Ikeda, Y., 1998. Hydrous and anhydrous alterations of chondrules in Kaba and Mokoia CV chondrites. *Meteoritics & Planetary Science* 33, 1139–1146. doi:10.1111/maps.12590.

Kimura, M., Yagi, K., 1980. Crystallization of chondrules in ordinary chondrites. *Geochimica et Cosmochimica Acta* 44, 589–602. doi:10.1016/0016-7037(80)90251-3.

Kita, N.T., Nagahara, H., Tachibana, S., Tomomura, S., Spicuzza, M.J., Fournelle, J.H., Valley, J.W., 2010. High precision SIMS oxygen three isotope study of chondrules in LL3 chondrites: Role of ambient gas during chondrule formation. *Geochimica et Cosmochimica Acta* 74, 6610–6635. doi:10.1016/j.gca.2010.08.011.

Klerner, S., 2001. Materie im frühen Sonnensystem: Die Entstehung von Chondren, Matrix und refraktären Forsteriten. Ph.D. thesis. Universität zu Köln.

Kong, P., Palme, H., 1999. Compositional and genetic relationship between chondrules, chondrule rims, metal, and matrix in the Renazzo chondrite. *Geochimica et Cosmochimica Acta* 63, 3673–3682. doi:10.1016/S0016-7037(99)00110-6.

Kurahashi, E., Kita, N.T., Nagahara, H., 2003. Bulk chemical compositions of individual chondrules in least equilibrated carbonaceous chondrites, in: The International Symposium, Evolution of Solar System Materials: A New Perspective from Antarctic Meteorites, pp. 63–64.

Lux, G., Keil, K., Taylor, G.J., 1981. Chondrules in H3 chondrites: textures, compositions and origins. *Geochimica et Cosmochimica Acta* 45, 675–685. doi:10.1016/0016-7037(81)90041-7.

MacPherson, G.J., Huss, G.R., 2005. Petrogenesis of Al-rich chondrules: Evidence from bulk compositions and phase equilibria. *Geochimica et Cosmochimica Acta* 69, 3099–3127. doi:10.1016/j.gca.2004.12.022.

Mahan, B., Moynier, F., Siebert, J., Gueguen, B., Agranier, A., Pringle, E.A., Bollard, J., Connelly, J.N., Bizzarro, M., 2018. Volatile element evolution of chondrules through time. *Proceedings of the National Academy of Sciences* 115, 8547–8552. doi:10.1073/pnas.1807263115.

Matsunami, S., Ninagawa, K., Nishimura, S., Kubono, N., Yamamoto, I., Kohata, M., Wada, T., Yamashita, Y., Lu, J., Sears, D.W.G., Nishimura, H., 1993. Thermoluminescence and compositional zoning in the mesostasis of a Semarkona group A1 chondrule and new insights into the chondrule-forming process. *Geochimica et Cosmochimica Acta* 57, 2101–2110. doi:10.1016/0016-7037(93)90096-F.

McCoy, T.J., Scott, E.R.D., Jones, R.H., Keil, K., Taylor, G.J., 1991. Composition of chondrule silicates in LL3-5 chondrites and implications for their nebular history and parent body metamorphism. *Geochimica et Cosmochimica Acta* 55, 601–619. doi:10.1016/0016-7037(91)90015-W.

Metzler, K., Pack, A., 2016. Chemistry and oxygen isotopic composition of cluster chondrite clasts and their components in LL3 chondrites. *Meteoritics & Planetary Science* 51, 276–302. doi:10.1111/maps.12592.

Misawa, K., Nakamura, N., 1988a. Demonstration of REE fractionation among individual chondrules from the Allende (CV3) chondrite. *Geochimica et Cosmochimica Acta* 52, 1699–1710. doi:10.1016/0016-7037(88)90238-4.

Misawa, K., Nakamura, N., 1988b. Highly fractionated rare-earth elements in ferromagnesian chondrules from the Felix (CO3) meteorite. *Nature* 334, 47–50. doi:10.1038/334047a0.

- Olsen, E.J., 1983. SiO₂-bearing chondrules in the Murchison (C2) meteorite, in: King, E.A. (Ed.), Chondrules and Their Origins, Lunar and Planetary Institute, Houston. pp. 223–234.
- Osborn III, T.W., 1971. Elemental abundances in meteoritic chondrules. Ph.D. thesis. Oregon State University.
- Pack, A., Russell, S.S., Shelley, J.M.G., Van Zuilen, M., 2007. Geo- and cosmochemistry of the twin elements yttrium and holmium. *Geochimica et Cosmochimica Acta* 71, 4592–4608. doi:10.1016/j.gca.2007.07.010.
- Palme, H., Spettel, B., Hezel, D., 2014. Siderophile elements in chondrules of CV chondrites. *Chemie der Erde-Geochemistry* 74, 507–516. doi:10.1016/j.chemer.2014.06.003.
- Patzer, A., Hezel, D.C., Bendel, V., Pack, A., 2018. Chondritic ingredients: II. Reconstructing early solar system history via refractory lithophile trace elements in individual objects of the Leoville CV3 chondrite. *Meteoritics & Planetary Science* 53, 1391–1412. doi:10.1111/maps.13084.
- Rubin, A.E., Pernicka, E., 1989. Chondrules in the Sharps H3 chondrite: Evidence for intergroup compositional differences among ordinary chondrite chondrules. *Geochimica et Cosmochimica Acta* 53, 187–195. doi:10.1016/0016-7037(89)90285-8.
- Rubin, A.E., Wasson, J.T., 1987. Chondrules, matrix and coarse-grained chondrule rims in the Allende meteorite: Origin, interrelationships and possible precursor components. *Geochimica et Cosmochimica Acta* 51, 1923–1937. doi:10.1016/0016-7037(87)90182-7.
- Rubin, A.E., Wasson, J.T., 1988. Chondrules and matrix in the Ornans CO3 meteorite: Possible precursor components. *Geochimica et Cosmochimica Acta* 52, 425–432. doi:10.1016/0016-7037(88)90098-1.
- Schneider, D.M., Symes, S.J.K., Benoit, P.H., Sears, D.W.G., 2002. Properties of chondrules in EL3 chondrites, comparison with EH3 chondrites, and the implications for the formation of enstatite

chondrites. *Meteoritics & Planetary Science* 37, 1401–1416. doi:10.1111/j.1945-5100.2002.tb01037.x.

Sears, D.W.G., Sparks, M.H., Rubin, A.E., 1984. Chemical and physical studies of type 3 chondrites—III. Chondrules from the Dhajala H3.8 chondrite. *Geochimica et Cosmochimica Acta* 48, 1189–1200. doi:10.1016/0016-7037(84)90055-3.

Tachibana, S., Nagahara, H., Mostefaoui, S., Kita, N.T., 2003. Correlation between relative ages inferred from ^{26}Al and bulk compositions of ferromagnesian chondrules in least equilibrated ordinary chondrites. *Meteoritics & Planetary Science* 38, 939–962. doi:10.1111/j.1945-5100.2003.tb00289.x.

Varela, M.E., 2019. Bulk trace elements of Mg-rich cryptocrystalline and ferrous radiating pyroxene chondrules from Acfer 182: Their evolution paths. *Geochimica et Cosmochimica Acta* 257, 1–15. doi:10.1016/j.gca.2019.04.025.

Varela, M.E., Sylvester, P., Brandstätter, F., Engler, A., 2015. Nonporphyritic chondrules and chondrule fragments in enstatite chondrites: Insights into their origin and secondary processing. *Meteoritics & Planetary Science* 50, 1338–1361. doi:10.1111/maps.12468.

Varela, M.E., Sylvester, P., Engler, A., Kurat, G., 2012. Nonporphyritic chondrules from equilibrated Rumuruti and ordinary chondrites: Chemical evidence of secondary processing. *Meteoritics & Planetary Science* 47, 1537–1557. doi:10.1111/j.1945-5100.2012.01417.x.

Wang, Y., Hsu, W., Li, X., Li, Q., Liu, Y., Tang, G., 2016. Petrology, mineralogy, and oxygen isotope compositions of aluminum-rich chondrules from CV3 chondrites. *Meteoritics & Planetary Science* 51, 116–137. doi:10.1111/maps.12590.

Wasson, J.T., Kallemeyn, G.W., Rubin, A.E., 2000. Chondrules in the LEW85332 ungrouped car-

bonaceous chondrite: Fractionation processes in the solar nebula. *Geochimica et Cosmochimica Acta* 64, 1279–1290. doi:10.1016/S0016-7037(99)00359-2.